AN ABSTRACT OF THE THESIS OF

Fujun Wang for the degree of Master of Science in Wood Science

presented on August 5, 2005

Title: Henry's Law Constants for Pollutants from the Wood Industry in Room Temperature Ionic Liquids

Abstract approved:

Redacted for Privacy

Mike R. Milota Kaichang Li

The emission of organic compounds from wood manufacturing facilities is an important regulatory concern due to their effects on ambient air quality. Control technologies, such as oxidizers and biofiltration, are used to remove organics from air streams; however, most removal technologies have high costs or cause additional negative environmental impact.

Room-temperature ionic liquids (RTILs) are liquid organic salts at ambient temperature and have the potential to be used to absorb organic compounds from airstreams. In this study, the Henry's Law constants were determined for methanol and α-pinene in four imidazolium-based RTILs (BMIN-BF_4, BMIN-PF_6, HMIN-PF_6, and OMIN-PF_6) and four phosphonium-

based RTILs (IL105, TBPD, THPD, and IL106). This was done in the dry condition and with 2% water content.

At 60°C, Henry's Law constants ranged from 0.04 to 0.13 for methanol and 0.01 to 0.04 for α-pinene (mole fraction units). The values increased as the temperature increased from 30°C to 90°C in accordance with the Van't Hoff equation. In some cases, the presence of water increased the Henry's Law constant.

Imidazolium-based ILs were unstable when heated, especially in the presence of water and are not recommended as absorbents. Of the ILs tested, THPD was best absorbent for both methanol and α-pinene.

The used RTILs containing contaminants can be recycled using high temperature and vacuum. The removal efficiency may reach 100%.

Henry's Law Constants for Pollutants from the Wood Industry in Room Temperature Ionic Liquids

by

Fujun Wang

A THESIS

submitted to

Oregon State University

In partial fulfillment of
the requirements for the
degree of

Master of Science

Presented August 5, 2005
Commencement June 2006

Master of Science thesis of Fujun Wang presented on August 5, 2005.

APPROVED:

Redacted for Privacy

Major Professor, representing Wood Science

Redacted for Privacy

Major Professor, representing Wood Science

Redacted for Privacy

Head of the Department of Wood Science and Engineering

Redacted for Privacy

Dean of the Graduate School

I understand that my thesis will become part of the permanent collection of Oregon State University libraries. My signature below authorizes release of my thesis to any reader upon request.

Redacted for Privacy

Fujun Wang, Author

ACKNOWLEDGEMENTS

I am grateful to Dr. Mike R. Milota and Kaichang Li for their help and guidance in my graduate study and research. I also greatly appreciate Dr. Milota's revisions and critical review of this thesis.

I am thankful to my dear husband, Yulin Zhao, for being with me and supporting me all the time.

I would like to express my appreciation to all the following colleagues in our research group for their assistance with this work: Paul Mosher and Michelle Schwartz.

This research was funded by the Department of Energy Agenda 2020 program. Grant # DE-FC07-03ID14432

TABLE OF CONTENTS

TABLE OF CONTENTS (Continued)

TABLE OF CONTENTS (Continued)

Page

TABLE OF CONTENTS (Continued)

TABLE OF CONTENTS (Continued)

LIST OF FIGURES

LIST OF FIGURES (Continued)

Figure Page

LIST OF TABLES

APPENDIX

Table page

HENRY'S LAW CONSTANTS FOR POLLUTANTS FROM THE WOOD INDUSTRY IN ROOM TEMPERATURE IONIC LIQUIDS

Chapter 1 Introduction

1.1 VOC and HAP emissions

The Environmental Protect Agency (EPA) defines volatile organic compounds (VOCs) as any compound containing carbon, excluding carbon monoxide, carbon dioxide, carbonic acid, metallic carbides or carbonates, and ammonium carbonate, which participate in atmospheric photochemical reactions [1]. They are a class of substances in which organic carbon is bonded to hydrogen or to other elements. Most VOCs have less than 12 carbon atoms [2]. Some VOCs are on the U.S EPA list of 189 hazardous air pollutants (HAPs) [3]. VOCs and HAPs are emitted nationwide. Based on 1996 data, processes that involve solvent utilization are responsible for 33% of the VOCs released to the atmosphere. The remaining 67% is provided by the following sources: transportation, fuel combustion, chemical product manufacturing, wood related product manufacturing, and other industrial processes [1].

The chemistry of VOCs in the atmosphere is complex. Degradation and transformation reactions may occur in the both gaseous and aqueous phases [4]. Harley et al. [5] concluded that some toxic compounds found in ambient air were formed in the atmosphere as oxidation products of other volatile organic compounds. For example, terpenes have been found to

react rapidly with ozone or hydroxyl or nitrate radicals to yield various organic compounds.

In recent years, VOC and HAP emissions have become significant environmental issues, which are receiving greater attention. VOC contamination in the air and water is a major health and ecological risk that can lead to tropospheric ozone formation, stratospheric ozone depletion, lung disease, and cancer [6]. EPA and State Agencies require more extensive removal of some VOCs and HAPs from industrial air streams since the implementation of the 1990 amendments to the Clean Air Act. These measures are important to the health of human beings, but will result in additional equipment and costs for industry.

1.2 Development of VOC and HAPs recovery technologies

The majority of VOC and HAP emissions are anthropogenic and dilute, which significantly increases the difficulty of VOC and HAPs recovery. Few technologies are currently available to control or recover pollutants from low concentration streams effectively.

Presently, there are two primary categories of treatment for removing VOCs, destruction and recovery [7]. Some treatment technologies use a combination of these. Generally, the destruction technologies include regenerative thermal oxidizers (RTOs), regenerative catalytic oxidizers

(RCOs), flaring, biofiltration, ultraviolet treatment and catalytic ozone oxidation. To date, RTOs, RCOs, and biofiltration are commonly used as control technologies in the wood composite industry [7, 8]. However, their operation can lead to high costs and negative environmental impact. Capture and concentration methods primarily include condensation, membrane separation, absorption, and adsorption.

Absorption of VOCs into selective solvents offers the opportunity for recovery in an environmentally sound process. Scrubbing of waste gases using selective solvents has been investigated [9, 10, 11]. The selection of suitable solvents for absorption was a key criterion. The absorption fluid selected must be recyclable. Otherwise, the absorption process would create a contaminated liquid stream. However, the volatility and toxicity of most solvents hampered further development of the technology.

It's very desirable to develop environmentally friendly, promising technologies capable of treating low concentration streams efficiently.

1.3 Room temperature ionic liquids

All the problems mentioned above are addressed by an absorption system containing a room-temperature ionic liquid (RTIL) as an absorbent. RTILs are liquids at ambient or far below ambient temperature that are comprised solely of ions [12]. RTILs, as "green solvents", are receiving much attention as replacements for organic solvents in industrial processes

due to their unique physicochemical properties [13]. Interest in this class of solvent stems from the properties they exhibit: 1) no measurable vapor pressure and thus create no VOCs, 2) high solubility of wide range of organic and inorganic compounds, 3) high thermal stability and high chemical inertness to VOCs and HAPs, and 4) facile variation in properties for specific applications through changing the structure of the ions [13, 14]. Due to their environmentally benign properties and increased concern on the negative impact from the traditional solvents, the research interests in RTILs increased drastically in the past few years. To date, RTILs have been utilized as excellent media for many applications such as reaction solvents for organic synthesis or polymerization, gas separation, liquid separation (extraction), electrolytes for batteries. [15].

As mentioned above, RTILs have very unique physicochemical properties, which make them ideal absorbents for the recovery of VOCs. Furthermore, the negligible vapor pressure of RTILs may promise the complete recycling of used RTILs without losses to the ambient air, which is both environmentally and economically desirable. In the wood industry, large amounts of VOCs such as terpenes, formaldehyde, and methanol are emitted into the environment when trees are processed into wood-based products [3]. In this study, VOCs and HAPs that could be recovered from wood industry exhaust will be targeted.

1.4. Objectives

The overall objectives of this study are

- ✧ to measure the Henry's Law Constant of representative VOCs in RTILs at various temperatures;
- ✧ to investigate the effect of various RTIL cations and anions on the absorption of VOCs and find the optimum absorbent for VOCs and HAPs;
- ✧ characterize the influence of water on the absorption;
- ✧ evaluate the removal of VOCs from RTILs under high temperature and vacuum

Chapter 2 Literature Review

2.1 VOC and HAP emissions

2.1.1 VOC and HAP emissions from wood composite industry

Wood-based composites are made from wood-based materials bonded together naturally or with synthetic adhesives using heat and pressure. The wood might be in the fibers, or may be larger particles, strands, veneer, or lumber. The nature of the wood raw material and the adhesive essentially determine the differentiated characteristics of the products. Wood-based composites may have more desirable properties than solid wood when processing variables are properly selected [16]. Wood-based composites have become increasingly specialized in recent years and are used in wide ranging applications. At present, plywood, laminated veneer lumber (LVL), hardboard, particleboard, and oriented strand board (OSB) are the major wood-based panel products on the market [16]. Adhesive bonding of wood components has played an essential role in the development and growth of the forest products industry and has been a key factor in the efficient utilization of our timber resource. However, manufacturing wood products especially results in VOC and HAP emissions.

VOC and HAP emissions have become a global issue due to their significant contribution to the air pollution and global warming. Compared

to other chemical process, the amount of VOCs released per unit of wood products may be relatively small, but as a cumulative annual amount, the total VOC emissions are quite significant [17]. According to the U.S. EPA, the total estimated VOCs released for the lumber and wood products industry is 41,423 short tons per year [17].

2.1.1.1 Reason for VOCs and HAPs emission from wood processing

VOC emissions from wood processing are thought to be mainly from the extractive compounds in wood, especially in heartwood, and the adhesive and additive in composites. The extractable constituents of heartwood include tannins, resins, fats, waxes, oils and other aromatic compounds [18]. In general, the portion of total extracts in wood varies from 3 to 9 percent for temperate species [18]. Therefore, more VOCs are released during drying and manufacturing softwood species than hardwood species. HAPs, mainly methanol, are formed as the wood is heated during processing.

The adhesive is an important and necessary constituent for bonding wood elements together to form wood-based composite products. The thermosetting adhesives including phenol-formaldehyde (PF), ureaformaldehyde (UF), melamine-formaldehyde (MF), and isocyanate, are mostly used in manufacturing wood-based composite products in industry

[16]. These chemical components in adhesives are the potential sources for VOC and HAP emissions, especially formaldehyde [17, 18].

2.1.1.2 Source for VOC and HAP emission in wood processing

The sources of VOC and HAP emissions at wood product facilities are mainly drying, resin blending, pressing, and finishing [19]. However, dryers and presses are the most important sources of emissions because high temperature accelerates the emissions. Emissions are mostly caused by evaporation and thermal degradation. Evaporation plays a major role from ambient to 200 °C as VOCs are given off with the water vapor [19]. Thermal degradation of wood components will contribute greatly to HAP emissions when temperature is increased above 200 °C due to breakdown of the of less-thermally-stable hemicelluloses between 200 °C and 280 °C [19, 20]. Formaldehyde will be a significant HAP when UF and PF resins are used and also can occur from the breakdown of wood components.

2.1.1.3 VOC and HAP emissions during wood processing

The actual composition of emissions from wood processing depends on the species of wood and processing conditions. Emissions from hardwood and softwood differ both in the nature and in the quantities of material evolved mainly due to their different extractive components [18].

Hardwoods emit principally degradation products that arise from the thermal breakdown of wood because the extractive content is small. These include VOCs, some of which are designated by the U.S. EPA as HAPs, such as methanol and formaldehyde [21]. Softwoods can release a larger quantity of VOCs, most of which are terpenes and other wood extractives [22]. Because softwood wood tissue is also subject to thermal breakdown during processing like hardwood, they also emit the same breakdown products as hardwoods [22].

Research on VOCs from wood processing has mostly centered on softwood species for two primary reasons. First, softwood species comprise over 83 percent of the lumber dried in the United States [23]. Nearly all solid structural lumber products, as well as most engineered wood products (i.e., plywood and other structural composite products), used in construction are derived from softwood species [16, 23]. And second, softwoods generally contain larger amounts of extractive material than hardwoods. Smaller total amount of VOCs and HAPs are likely from hardwood processing.

Processing conditions, such as moisture content, wood particle size, temperature, pressure, storage time of the raw material, types of adhesives and additives also play significant roles in determining the VOC and HAP emissions from the manufacturing of wood-based composite products [22].

Although the VOC composition changes with both species and drying conditions, methanol and formaldehyde are the two major HAPs

emitted from both hardwood and softwood. Among the HAPs emitted, methanol, formaldehyde, acetaldehyde, acrolein, phenol and propionaldehyde are the HAPs of most concern to the EPA [24]. α-pinene and β-pinene are the most notable VOCs released from most softwoods and α-pinene can be oxidized by air to ringed compounds with aldehydes, ketones and hydroxyl groups [3, 24]. As a result, 25 or 30 compounds in the terpene family might be detected in dryer exhaust [25]. Nonterpene VOCs emitted from wood include acids such as formic, acetic and propionic. Total organic emissions from softwood lumber are 0.25 to 3 pounds per 1,000 board feet and 0.5 to 4 pounds per ovendry ton are released from dryers [3]. In the late 1990s, the National Council of the Paper Industry for Air and Stream Improvement (NCASI) tested emissions at 29 wood product mills to provide emissions data which could be used by the industry and EPA in the development of the Maximum Achievable Control Technology (MACT) rule [26]. Concentrations measured during this study are listed in Table 1. The major VOCs, methanol, α-pinene and formaldehyde, are all emitted at low concentrations.

Table 1. The concentrations of some VOCs mainly based on emissions from press and dryer [26].

VOCs&HAPs Products	Methanol (ppm)	α-pinene (ppm)	Formaldehyde (ppm)	THC (ppm)	Gas Temp. (^{0}F)
OSB	2.0-90	7.8-50	2.4-45	130-1200	100-190
Plywood	5.5-21.7	66.6-249.0	4.4-20.8	1814-5090	290-330
Particleboard	4.5-110	13-15	1.1-43	120-800	140

2.1.2 Regulations for VOC and HAP emissions from industry

Environmental concerns arise because VOCs are potential precursors for photochemical formation of ozone, other atmospheric oxidants, and aerosols in troposphere. Some VOCs deplete ozone in stratosphere and some such as formaldehyde, are known or suspected to have adverse effects on human health [5]. These factors have resulted in strict regulations by U.S. EPA and State Agencies for VOC and HAP discharges. The wood-based panel industry is facing a new challenge, the further abatement of VOCs and HAPs, and is searching for novel techniques for reducing VOCs and HAPs.

Air pollution concerns have existed since coal was burned as fuel 500 years ago. However, the first air pollution control regulation in the

United States, the Air Pollution Control Act, was not developed until 1955 [27]. This Act required the U.S. Public Health Service to assist communities in reducing the formation of photochemical smog. Clean Air Acts (CAA) in 1963 and 1967 provided for a better understanding through research. The U.S. EPA was created in 1970 by executive order [27]. A Clean Air Act, also passed in 1970 and amended in 1977, authorized the EPA to establish the National Ambient Air Quality Standards (NAAQS) for seven criteria pollutants including particulate matter PM_{10}, VOCs sulfur oxides, nitrogen dioxide, carbon monoxide, ozone, and lead. Also, The CAA directed each state to develop a state implementation plan to achieve the NAAQS. The 1990 amendments to the CAA used approaches for reducing pollution that were different from the past legislation in that market-based principles and emission banking and trading were introduced [27]. Another result of the 1990 CAA are uniform standards that regulate the release of HAPs from many industries. These are known as the Maximum Achievable Control Technology (MACT) regulations [28]. The MACT rule for the wood industry provides for six compliance options. Add-on control technologies must be used on certain types of dryers and presses at major sources to reduce total hydrocarbon (THC) emissions by 90 percent, reduce methanol emissions by 90 percent, reduce formaldehyde emissions by 90 percent, limit the concentration of THC in the outlet of the add-on control device to 20 parts per million by volume dry basis (ppmvd), limit the concentration of methanol in the outlet of the add-

on control device to 1 ppmvd, or limit the concentration of formaldehyde in the outlet of the add-on control device to 1 ppmvd [29, 30]. Technologies capable of treating low concentration gas streams are needed due to these stringent regulations.

2.1.3 Control technologies for VOC and HAP emissions

As mentioned previously, RTOs, RCOs, biofiltration and absorption are most commonly used control technologies for VOC and HAP emissions in wood-based panel industry. Both the advantages and disadvantages are discussed below.

2.1.3.1 RTOs and RCOs

Thermal oxidation (TO), or thermal incineration, is the process of oxidizing combustible materials using a high temperature for sufficient time to convert the pollutants to carbon dioxide and water [8, 31]. Processing conditions such as time, temperature, turbulence (for mixing) and the amount of oxygen significantly affect the rate and efficiency of the combustion process [8, 32]. Operating temperatures range from 650 ºC to 1100 ºC (1200–2000°F) and gas residence times are typically 1 second or less [8]. Natural gas is used as fuel. The typical equipment for thermal oxidation technique is sketched in Figure 1.

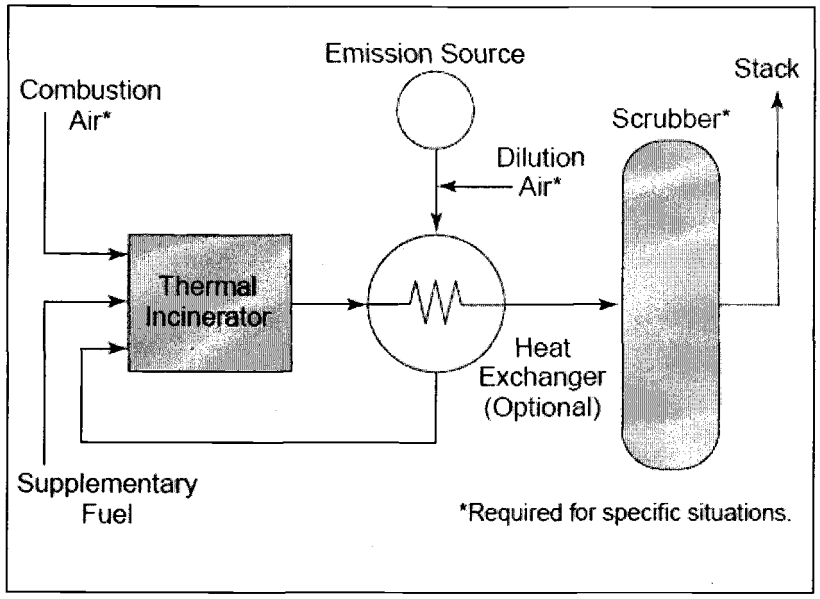

Figure 1. A thermal oxidizer incorporates regenerative energy recovery [8].

Regenerative Thermal Oxidation (RTO) units are distinguished from thermal oxidation only by their ability to recover heat at high efficiency. A RTO uses a high-density media such as a ceramic-packed bed which is still hot from a previous cycle to preheat an incoming waste gas stream containing VOCs and HAPs [8]. Therefore, RTOs generally have lower fuel requirements because of higher energy recovery (up to 95%) compared to TOs.

Regenerative catalytic oxidations (RCOs) operate similarly to RTOs. The primary difference is the use of a catalyst, which has the effect of increasing the oxidation reaction rate, thus allowing the reaction to occur at a lower temperature than is required for thermal ignition [31, 32]. The maximum operating temperature ranges from 540°C to 675°C (1,000–1,250°F) for RCOs. RCOs, therefore, use less energy than RTOs [8, 31].

In general, metal oxides or precious metals, such as platinum and palladium are used as catalysts for VOC or HAP abatement and they have a longer service life and are more resistant to poisoning and fouling than less-expensive base-metal catalysts, such as manganese dioxide [8].

RTOs and RCOs are proven to be a method for destroying VOC/HAPs, with destruction efficiencies up to 99.9999% [8]. They can be used to reduce emissions from almost all VOC and HAP sources, including process exhaust vents, storage tanks, treatment, and storage and disposal facilities. However, they are not well-suited to exhaust streams with highly variable flowrates, which cause the combustion chamber temperature to fall and the destruction efficiency to drop [8, 32].

2.1.3.2 Biofiltration

Biofiltration utilizes microbes to breakdown VOCs and HAPs and thus offers an environmentally attractive alternative to RTOs and RCOs [33]. The key component of a biofiltration system is a bed (Figure 2), made of natural materials such as soil and bark that is maintained at high humidity by continuously supplying water through sprayers [7, 8]. The moisture level is very important to the proper functioning and efficiency of a biofilter because the degradation processes of VOCs or HAPs are exothermic and tend to dry the filter beds. Typically, the organic pollutants in the waste gas stream dissolve in water and then are converted by

microorganisms to water and dioxide in the biolayer. The type of microorganism used depends on the type of VOCs/HAPs treated.

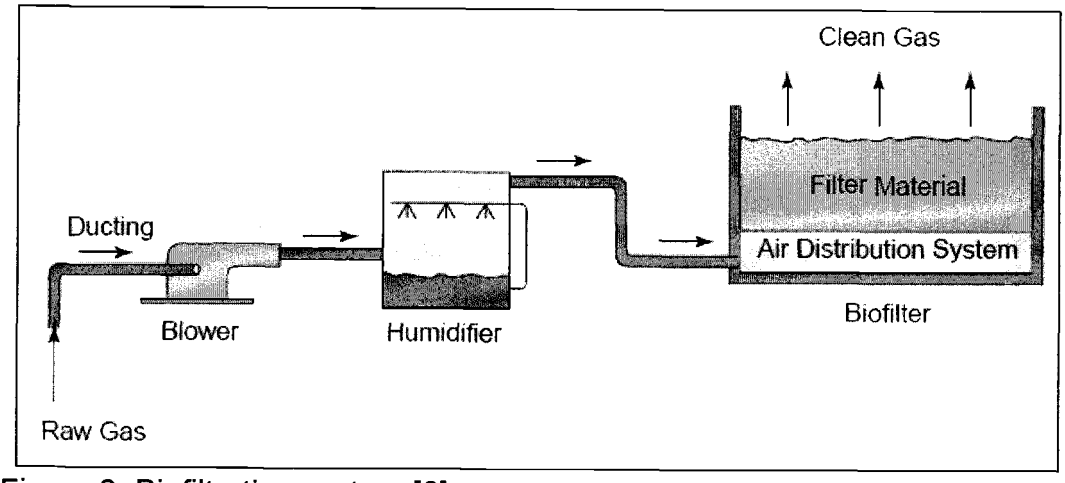

Figure 2. Biofiltration system [8].

In general, water-soluble, oxygenated compounds with low molecular weight are good candidates for biofiltration. Aldehydes, ketones, alcohols, ethers, esters and organic acids degrade rapidly in biofilters. However, halogenated hydrocarbons and polyaromatic hydrocarbons do not. For easily degradable compounds, removal efficiencies have been demonstrated to be greater than 90% [8].

Other less common methods for removal of VOCs and HAPs include adsorption, which employs activated carbon, silica gel, polymeric beads, or zeolites as adsorbents, and degradation with plasma (or corona), and ultraviolet light (UV) [31]. Adsorption of VOCs and HAPs onto activated carbon, silica gel, polymeric beads, or zeolites is a non-selective process.

Moisture from the gas will also be adsorbed onto these materials, thus lowering the efficiency of the removal of VOCs and HAPs [34]. Moreover, large molecular compounds such as fatty acids and resins will permanently block the adsorption sites and make regeneration of the adsorbents difficult. Other techniques, such as degradation of VOCs and HAPs with plasma, corona, or UV are still in development.

2.1.3.3 Absorption

Gas absorption or scrubbing is the unit operation in which one or more soluble components of a gas mixture are dissolved in a liquid. The absorption may be a purely physical phenomenon or may involve reaction among the constituents in the liquid solution. The reverse operation called stripping or desorption is employed to transfer one or more volatile components from liquid mixture into a gas [35]. Absorption systems are often used to separate gaseous streams containing high concentrations of organics, especially water-soluble compounds such as methanol, ethanol, isopropanol, butanol, acetone, and formaldehyde. It is widely used to abate VOC and HAP emissions from industry, especially for natural gas purification [8, 31].

However, several factors limit the use of absorption as the primary control technique for VOCs and HAPs recovery. One factor is the availability of a suitable solvent for the VOCs and HAPs. To date, water

and high boiling point mineral oils or other petroleum oil are most common used. Another factor is the availability of vapor/liquid equilibrium data, usually as Henry's Law Constants, for the specific organic/solvent system are necessary for the design of absorber systems. However, they are not readily available for uncommon organic compounds. In addition, the desorption efficiency and disposal of pollutants from absorbents have to be considered to avoid creating a second contaminated stream. In most cases, VOC/HAP is desorbed from the absorbent at elevated temperatures and/or under vacuum so that the scrubbing liquid containing the VOCs and HAPs is regenerated for reuse again. The VOC or HAP is then recovered as a liquid in a condenser.

2.1.4 Issues associated with current VOC and HAP destruction technologies

Sauer et al. [36] investigated the environmental tradeoffs associated with various emission control technologies currently used in the wood products industry. They concluded that the use of RTOs and RCOs resulted in greater life cycle burdens for energy, solid waste, greenhouse gas, CO, NO_x, SO_x, and other emissions even though VOC and HAP emissions and particulate emissions were reduced efficiently by RTOs and RCOs destruction technologies. In addition, RTOs and RCOs need high capital costs, high installation costs, high utility operating costs and high maintenance costs, for moving parts and catalysts [7, 32].

Biofiltration creates no green house gases due to the combustion of fuel. It is an environmentally benign technology for VOC and HAP destruction. However, the biofilter bed lifetime is limited to two to five years even though occasional washing of the bed can extend its life in some cases [8, 36]. In addition, the temperature of the exhaust from wood products facilities can be high enough to inhibit the growth of microbes in biofilters, thus reducing the rate at which microbial degradation of the VOCs occurs. Biofilters are also difficult to operate because mill shutdowns disturb the life cycle of the microbes [34, 36].

Any destructive treatment, such as RTOs, RCOs, and biofiltration, eliminates the possibility of chemical recovery [7]. The absorption of VOCs and HAPs into solvents clould be a reversible process and permit chemical recovery. Presently, much research is focused on scrubbing of waste gases using selective solvents [10, 11]. The commonly used absorbents such as high-boiling mineral oils and petrol oils produce VOC emissions at high operating temperature [11]. This limits their use for absorption in industry. Therefore, solvents with negligible vapor pressure, thermal and chemical stability, and high solubility to large range of VOCs are desirable for the absorption technology of the future.

2.2 Room Temperature Ionic Liquids

2.2.1 Introduction

Room temperature ionic liquids (RTILs) are organic salts that are liquids at ambient temperature. In the early 1990s, the first air- and water-stable ionic liquids with anions hexafluorophosphate and tetrafluoroborate were prepared [37]. In recent years, RTILs have received increased attention. Due to their unique physiochemical properties, RTILs appear to be attractive replacements for traditional organic solvents. RTILs are referred to be "green" designer solvents [38, 39, 40]. Although imidazolium based ILs are the most widely available, pyridinium-, ammonium- and phosphonium-based ILs are also in use [41].

2.2.2 Properties and Applications

RTILs offer a variety of physicochemical properties that make them attractive replacements for traditional organic solvents. Some of these properties are common to all ionic liquids. The negligible vapor pressure of RTILs is very desirable in many applications, especially at high temperature. This property is significant when addressing the health and safety concerns associated with many traditional solvents. Negligible vapor pressure means solvent evaporation is eliminated, reducing the need for respiratory protection and exhaust systems. Furthermore, their non-volatility allows RTILs to be used at elevated vacuum and temperature

without loss. A range of separation techniques such as distillation and vacuum stripping could be used to recycle used RTILs. These are not possible when using low-boiling organic solvents [42].

The ability to dissolve a wide range of organic and inorganic compounds makes RTILs excellent solvents. This is important when dissolving disparate combinations of compounds. Presently, research using RTILs as solvents has been focused on homogeneous catalysts because reactions tend to proceed faster and with more control when they take place in solution [43, 44]. RTILs dissolve both the reactants and catalysts, which make reactions more efficient. The easy recycling of catalyst and byproducts is a further benefit.

Generally, RTILs remain as liquids to 300 °C and have high thermal stability. Most traditional solvents will either freeze or boil across such a large temperature range [34, 44]. This wide range of thermal stability allows for tremendous kinetic control of chemical process. Meanwhile, it is also very important for temperature-dependent separation techniques such as extraction and crystallization. For example, a natural product can be extracted into an IL at 150 °C and precipitated by cooling to room temperature [37].

Another fundamental property of RTILs is ion conductivity, which makes them good electrolytes. RTILs can be used to replace the traditional solvent-based electrolytes, which are prone to corrosion, leakage, volatility, and flammability. Other advantageous properties that

RTILs offer over traditional solvents include enhanced enzyme lifetime, improved chemo-selectivity even for heterogeneous reaction, easier catalyst recovery, and recycling as reaction solvents or media [15, 37].

Based on these unique properties, RTILs still have many other potential applications rather than as reaction solvents. RTILs can be used as absorbents for gas separations. Many RTILs are hygroscopic and thus can efficiently remove water vapor from a gas stream [45, 46]. CO_2 has remarkably high solubility in some RTILs [42, 45]. Therefore, RTILs may be desirable absorbents for VOCs and HAPs. Many RTILs are excellent solvents for a wide variety of both polar and nonpolar compounds [42]. This property allows for RTILs potential absorbents for both polar and nonpolar compounds.

RTILs are typically comprised of combinations of bulky organic cations and organic or inorganic anions, invariably possessing a high degree of asymmetry that frustrates packing and thus inhibits crystallization. This explains the fact that RTILs are liquid instead of solid at room temperature as other conventional salts such as sodium chloride [15]. Generally, anions that form RTILs are weakly basic organic or inorganic compounds that have a diffuse negative charge [15]. Anions have a strong influence on the viscosity of RTILs, though factors affecting the viscosity are still poorly understood [15, 47]. Also, anions dramatically affect water miscibility. Subtle changes in the nature of the anion, such as a change from the tetrafluoroborate [BF_4^-] to the hexafluorophosphate

anion [PF_6^-] can significantly change the hydrophilicity. Anion [BF_4^-] is more hydrophilic than [PF_6^-] [45].

Both the cations and the substituent groups (R-group) on cations have important effects on the physicochemical properties of RTILs. However, the selection of different anions has a more significant and wide-ranging effect on the properties of RTILs than does a variation in cation and R-group [37, 47]. Generally, cations that produce low melting points are organic species with high asymmetry.

2.2.3 RTILs as "green designer" solvents

RTILs have been described as green designer solvents, where "green" means environmental friendly properties and "designer" indicates that their properties can be adjusted to suit the specific requirements of a particular process [15, 40]. Physicochemical properties such as melting point, viscosity, density, hydrophobicity and solvation can be varied at will by simple changes to the structure of cations, R-group, and anions [40, 48]. Generally, the melting points of RTILs increase with increasing substituents chain length [49, 50]. Meanwhile, with an increase in the number of carbon atoms in alkyl chain, viscosity initially decreases from methyl- to ethyl-group and then increases with further increase in the alkyl chain length [50]. In addition, 1-octyl-3-methylimidazolium tetrafluoroborate ([Omim][BF_4^-]) will accept more water than 1-butyl-3-methylimidazolium

hexafluorophosphate ([Bmim][PF_6^-]) because the anion [BF_4^-] is more hydrophilic [45].

As shown in Figure 3, the various combinations of cations, substituents, and anions promise a wide range of tunable properties for specific applications. To date, numerous attempts including combinations of new anions, cations and substituents have been made to prepare novel RTILs and understand their characteristics.

Incorporating a capacity for selective interactions with substrates can create task-specific ILs capable of accomplishing specific tasks. Bates et al. successfully designed a task-specific IL (TSIL) which could readily and reversibly sequester CO_2 [51]. Moreover, some new TSILs have proven useful in both synthesis and separation applications [52, 53].

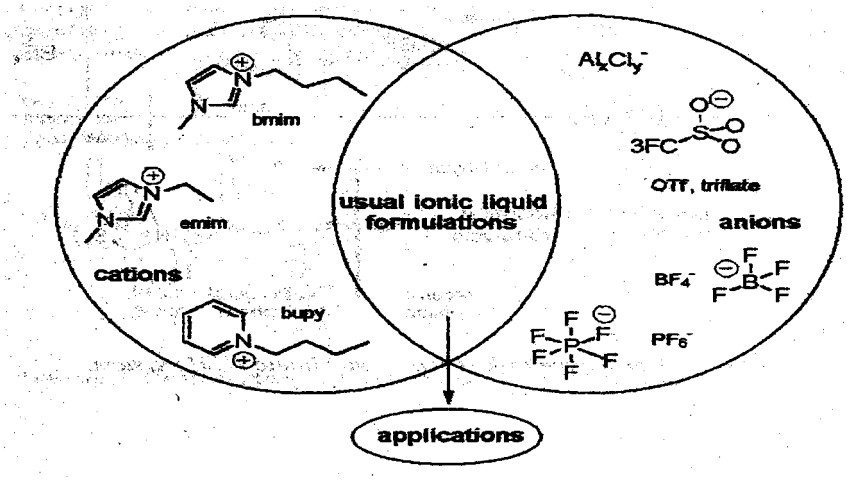

Figure 3. Formulations of a variety of RTILs by different cations, anions and substituents [48].

2.2.4 Imidazolium-based RTILs

RTILs based on imidazolium salts with anions such as [BF_4^-] and [PF_6^-] exhibiting a wider range of chemical and electrochemical applications, are a major breakthrough in the chemistry of ionic liquids [48]. Based on the number of R-groups on the cation, imidazolium-based ILs can be categorized into three types including monosubstituted, disubstituted, and trisubstituted imidazoliums. The major structures for these are shown in Figure 4.

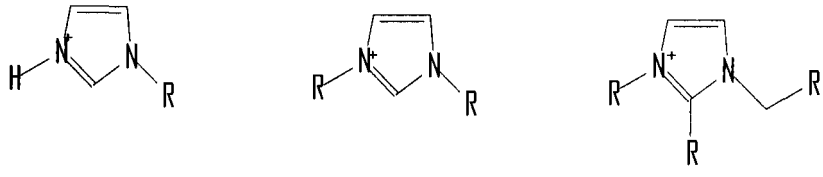

Figure 4. The structures of monosubstituted, disubstituted and trisubstituted imidazoliums.

Salts based on the 1,3 dialkylimidazolium cation represent the largest group of room temperature ionic liquids currently available because they are easily prepared and synthesized and have attractive properties [54]. Fredlake et al. [49] investigated the thermophysical properties of 13 imidazolium-based RTILs and provided fundamental understanding for the design of this type of RTIL. The physical and electrochemical properties of air-stable 1,3-dialkyl imidazolium-based RTILs have been extensively studied for their application as reaction media and electrolytes for batteries

[15]. These imidazolium-based RTILs possess several properties such as non-volatility, non-flammability, and high thermal and electrochemical stability, which make them attractive alternatives to traditional volatile solvents and nonaqueous electrolytes. Visser et al. [52] has studied the characterization of hydrophilic and hydrophobic imidazolium-based RTILs as alternatives to VOCs for liquid-liquid separations, providing detailed knowledge of the solvents' physical properties for RTILs comprised of the 1,3 dialkylimidazolium cation.

2.2.5 Phosphonium-based RTILs

Phosphonium-based RTILs are comprised of tetraalkylphosphonium, ($[PR_1R_2R_3R_4]^+$) as cations and various anions such as cyanide dicyanamide ($N(CN)_2$) or sulfonate derivatives [55]. The alkyl groups, R_n, generally are large and not all the same as shown in Figure 5.

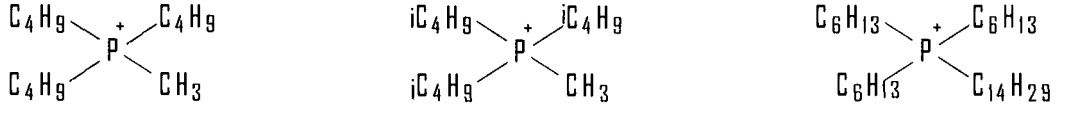

Figure 5. The typical cation structures of phosphonium-based RTILs.

The numerous RTILs that can be synthesized using various R-groups and anions increase the fine tunability of the resulting properties such as their melting point, viscosity and electrochemical properties. The

large phosphonium cations can combine with relatively large anions to make viscous but free flowing liquids [41]. The phosphoniums lack the weakly acidic ring protons, which are more common in imidazolium cations – a limitation when strongly basic anions are used, therefore, the quaternary phosphonium salts have been reported to be more chemically stable than nitrogen-based cations [41].

Although the phosphonium-based RTILs have not received as much attention as the more common imidazolium and other nitrogen-containing RTILs, they have been used extensively in several areas of chemistry for many years, such as catalysis, phase transfer reactions, and extractions [56, 57]. A number of these phosphonium salts with desired anions were synthesized with nearly all being liquids at and well below room temperature. They are stable up to 400 °C in some cases [41].

2.3 Recovery of VOCs and HAPs using RTILs as absorbents

2.3.1. Basics of RTILs as absorbents

Due to their unique physiochemical properties, RTILs have the potential to be media in separation technologies. RTILs have been used as solvents for liquid-liquid extraction, gas-liquid extraction, and gas separation [15, 37, 46, 58]. There is increased interest in using ionic liquids to replace volatile organic solvents for gas separations.

Scovazzo et al. [58] successfully separated CO_2 from N_2 using RTIL [Bmim][PF_6]. Anthony et al. [46] reported the solubility of carbon dioxide, ethylene, ethane and methane in [Bmim][PF_6^-] and concluded that CO_2 was quite soluble in [Bmim][PF_6^-] followed by ethylene, ethane, and methane. This study is very important in evaluating RTILs as media for reactions involving gases. Baltus et al. [59] obtained the Henry's constants of CO_2 in nine different ionic liquids which help in understanding the role of chemical structure on the separation capabilities of RTILs. CO_2 has notably greater solubility in the ionic liquid having the fluorine-substituted anion as compared to the corresponding ionic liquid with a nonfluorinated anoin.

Crosthwaite et al. [60] studied the liquid phase behavior of imidazolium-based ionic liquids with alcohols and concluded that the effect of alkyl chain length on the cation and the choice of anion have significant effects on the solubilities of alcohols due to the coulombic and van der Waals interaction between the RTILs and alcohols. [Bmim][BF_4^-] is completely miscible with methanol and ethanenitrile [60]. With regard to the waste gases from wood composite industry, methanol is an important pollutant. Therefore, these studies about the relationships between RTILs and alcohol indicated that RTILs might be good absorbents to VOCs and HAPs.

2.3.2. Effect of water

Although water stable, some RTILs are hygroscopic, so the uptake of water vapor in RTILs is an important concern [45]. The presence of water may significantly change the properties of RTILs such as viscosity, density, and ion conductivity. Seddon et al. [61] pointed that the anion has a greater effect on water miscibility compared to the alkyl chain length on the cation.

Exhaust gases from the wood dryers and presses normally have a high moisture content. Water can be present in RTILs due to ineffective drying or due to absorption from the ambient air. The presence of water in RTILs is a concern because it may alter their absorbing capacity of VOCs and HAPs in the RTILs.

2.3.3. Recycling of used RTILs

A RTIL used for adsorption system must be recycled or a contaminated liquid stream is created. RTILs have no measurable vapor pressure, which allows for the separation between RTILs and contaminants using distillation and vacuum with negligible loss [45]. Ionic liquid/organic mixtures can be separated by application of CO_2 at pressures that induce a phase split, thereby providing a means of recovering the ionic liquid from

mixtures used in an extraction process [42]. Bates et al. desorbed CO_2 from RTIL upon heating 80-100 °C for several hours under vacuum [51].

2.4 Solid phase microextraction and gas chromatography

Solid Phase Microextraction (SPME) is an innovative technology that allows solventless sampling of volatiles and semivolatiles from a wide variety of matrices. It has been used to measure drugs and their metabolites in body fluids, volatile organic compounds (VOCs) in liquids, and explosive residues from solid samples [63]. The tool for SPME is a fiber coated with a liquid (polymer), a solid (sorbent), or a combination of both. The fiber coating removes the compounds from a sample by absorption in the case of liquid coatings or adsorption in the case of solid coatings. Compared to conventional sample preparation techniques, SPME provides fast, easy to use, and inexpensive sampling, and eliminates the use of organic solvents [64]. The first application of SPME was to evaluate pollutants in water [64]. To date, SPME has been successfully applied in numerous environmental, food, flavor, pheromone, pharmaceutical, clinical and forensic applications, and especially for quick screening of the volatile composition of a various range of products. Koziel et al. [65] pointed out that SPME is the fastest extraction technique for air sampling at typical airborne VOC concentrations. Presently, the poly(dimethylsiloxane) (PDMS) coating is one of the most widely used

coatings for extracting volatile analytes from environmental samples via absorption [65]. The sensitivity of solid (or mixed-phase) SPME coatings, such as divinylbenzene (PDMS/DVB) and Carboxen/PDMS, are much higher compared to PDMS for extracting VOCs.

SPME can be used in conjunction with gas chromatography (GC) as an innovative analytical method. The analytes are extracted from a variety of matrixes by partitioning them from a liquid or gas sample onto a stationary SPME adsorbent. The extracted analytes can be thermally desorbed in the injector of the GC and subsequently swept onto the column where they are separated [66]. The technique has been successfully used for the analysis of a wide range of volatile and semivolative components, where the traditional sample preparation methods, such as steam distillation and direct solvent extraction, are time-consuming and difficult to operate.

Sostaric et al. [66] found the SPME-GC technique to be suitable for analyzing the volatile components that exsit in vanilla extracts and flavorings. Spinhirne et al. [67] analyzed the VOCs in bovine breath using the SPME-GC method, and showed it to be a useful diagnostic tool for animals and humans. The concentrations of some VOCs such as acetic acid and formaldehyde from particleboard, medium density fibreboard (MDF) and engineered wood also have been studied. Lattuati-Derieux et al. [68] investigated the VOCs from paper materials by the SPME-GC technique and he concluded that SPME was a non-destructive, non-

contact method, which seemed especially suitable for investigating volatile compounds emitted.

2.5 Henry's Law Constant

Chemical transfer between environmental compartments plays a key role in both the control and reduction of contaminants. The solubility of a gas in an aqueous phase depends on temperature, the partial pressure of the gas over the liquid, the properties of the liquid and of the gas. The gas-liquid partitioning equilibrium constant, better known as the Henry's constant (K_H or H) is a crucial parameter in order to determine the solubility of chemicals into aqueous phase [62]. There are several ways of describing the Henry's law constant. Usually, it is defined as:

$$K_H = \frac{P_g}{C_L'} \quad \text{(atm·L / mol)} \tag{1}$$

$$\text{or } H = \frac{C_g}{C_L} \quad \text{(dimensionless)} \tag{2}$$

where P_g = gas partial pressure

C_L' = concentration of contaminant in gas (mole/L)

C_g = concentration of contaminant in gas (mole/mole)

C_L = concentration of contaminant in liquid (mole/mole)

R = universal gas constant (atm·L /mol·K)

T = temperature (K)

Based on expressions (1) and (2), Henry's constant is inversely proportional to gas solubility, which means a high value of K_H or H corresponds to the low gas solubility into aqueous phase.

Therefore, the solubility of contaminants into each RTIL can be determined by measuring the Henry's constants.

2.6 Temperature dependence of Henry's Law Constant

The laws of thermodynamics (Van't Hoff equation) predict that Henry's law constant varies with temperature and pressure. At a constant pressure, the temperature dependence of Henry's law constant can be expressed as equation 3 [69].

$$H_i = \exp\left(\frac{B_{H_i}}{T} - A_{H_i}\right) \tag{3}$$

where T is the absolute temperature (K) and A_{H_i} and B_{H_i} are constants depending on the nature of solvent-solute combination. Over a narrow temperature range in which the heat of vaporization of the solute from solvent remains constant, there is a linear relationship between the natural logarithm of the Henry's law constant for a given compound and the reciprocal of the absolute temperature [69].

Chapter 3 Experiment

3.1 Materials

3.1.1 Representative compounds

Methanol and α-pinene, were selected as representative of the contaminants emitted during the drying and pressing of wood. They are significant VOCs released during drying and pressing. Also, these compounds should have very different absorption properties. Methanol is a small, polar molecule and α-pinene is a large, non-polar molecule. Analytical grade methanol and α-pinene were purchased.

3.1.2 Imidazolium-based RTILs

Four imidazolium-based room temperature ionic liquids (RTILs), BMIM-PF_6, HMIM-PF_6, OMIM-PF_6, and BMIM-BF_4, were selected (Table 2). The first three RTILs selected have the same anion, but have an alkyl group of increasing length on the cation which allows for the investigation of effect of substitution. Another RTIL, BMIM-BF_4 was chosen because it has a different anion so that the effects from the anion can be studied. All four are commercially available and were provided by Cytec. Inc.

Table 2. Properties of imidazolium-based RTILs.

RTILs	BMIM-PF_6	HMIM-PF_6	OMIM-PF_6	BMIM-BF_4
Formula	$C_8H_{15}N_2P\ F_6$	$C_{10}H_{19}N_2P\ F_6$	$C_{12}H_{23}N_2P\ F_6$	$C_8H_{15}\ N_2BF_4$
M (g/mol)	284.2	312.4	340.3	226.0
Density (g/mL)	1.38	1.28	1.25	1.20
Melting point (°C)	6.5	-74	------	-71
Structure	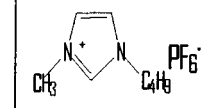	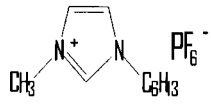	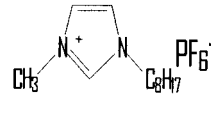	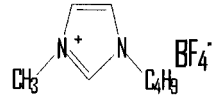

3.1.3 Phosphonium-based RTILs

Four phosphonium-based RTILs were selected after encountering problems with the imidazolium-based RTILs. These four RTILs are trihexyl(tetradecyl)phosphonium dicyanamide (IL105); Tri-iso-butyl(methyl)phosphonium tosylate (IL106); Tributyltetradecylphosphonium dodecylbenzenesulfonate (TBPD); and Trihexyltetradecylphosphonium dodecylbenzenesulfonate (THPD). The selection of these four RTILs was based on the varieties of cations, anions, and substitution, which may change the absorption capability of RTILs. TBPD and THPD have the same anion and different alkyl groups substituted onto the cation (Table 3).

IL105 and THPD have the same substituent and cation, but different anions. Among these four RTILs, IL105 and ILI06 were provided by Cytec. Inc. However, TBPD and THPD were not commercially available and were synthesized in our lab by anion exchange reactions, which took place at room temperature and neutral pH. Tributyltetradecylphosphonium chloride and trihexyltetradecylphosphonium chloride were used as starting material for each reaction, respectively.

Table 3. Properties of phosphonium-based RTILs.

RTILs	IL105	IL106	TBPD	THPD
Formula	$C_{32}H_{68}P$ C_2N_3	$C_{20}H_{37}P$ S O_3	$C_{12}H_{23}N_2P$ F_6	C_8H_{15} N_2BF_4
M (g/mol)	549.9	388.5	725.2	809.3
Density (g/ml)	0.89	0.89	0.95	0.93
Melting point (°C)	------	------	------	------
Structure	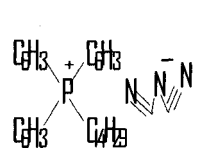	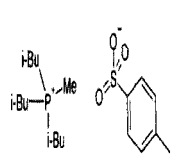	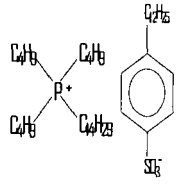	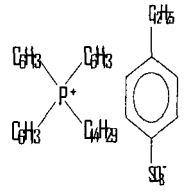

3.2 Imidazolium-based RTILs

3.2.1 Overview of experimental procedures

The experimental procedures for determining Henry's constants for the methanol and α-pinene in imidazolium-based RTILs are shown in Figure 7. The general procedure is to bring gas containing a known concentration of contaminate into contact with an ionic liquid by bubbling through an impinger. The liquid is then sampled after the equilibrium is reached in impinger. The contaminate concentration in the liquid is determined by headspace analysis. Detailed information about these procedures is in the following sections.

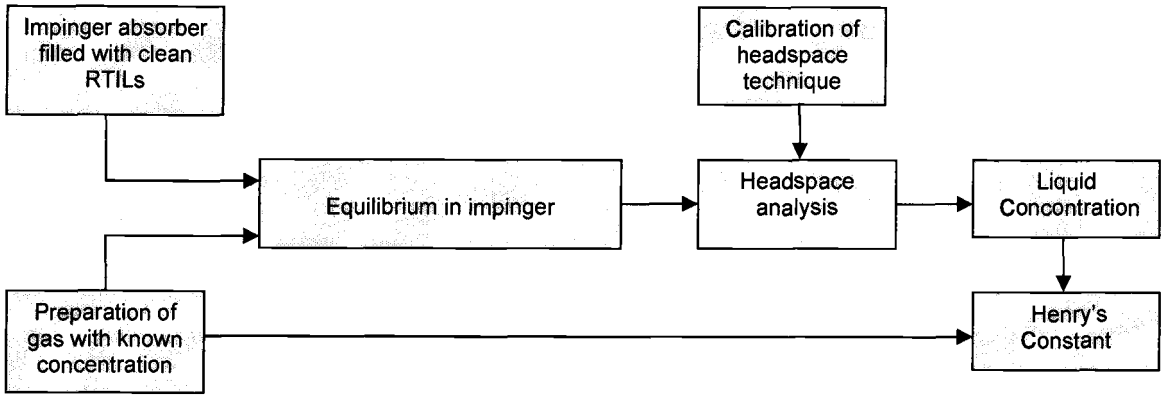

Figure 7. Experimental procedures for determining Henry's constants for contaminates in imidazolium-based RTILs.

3.2.2 Preparation of gases

Gases with a known concentration of contaminant were prepared in the laboratory from air and the contaminant in liquid form. Then concentrations were verified gravimetrically based on the change in liquid mass over time.

3.2.2.1 *Preparation*

Air containing methanol and α-pinene in known concentrations were generated in the lab as shown in Figure 2.

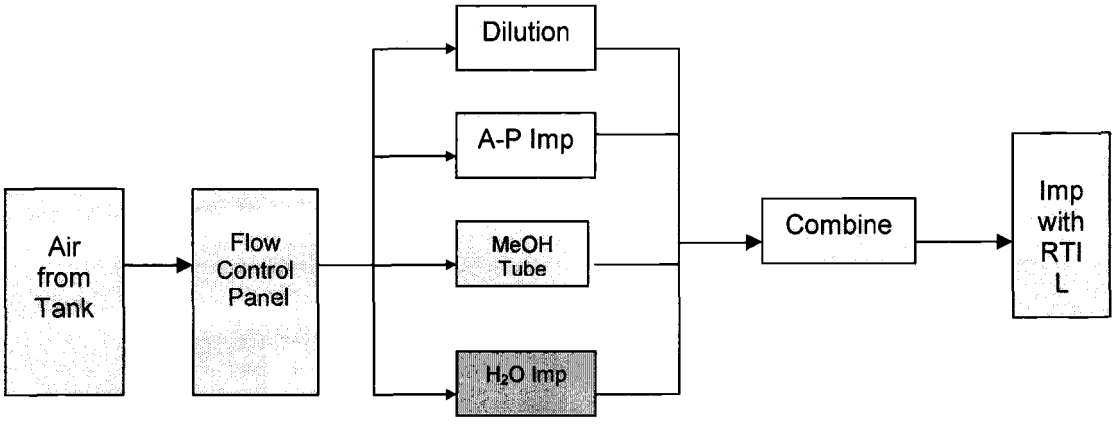

Figure 8. Laboratory equipment for generating air containing known concentrations of methanol and α-pinene.

Clean compressed air goes through a flow control panel consisting of four independent flow meters and control valves. The panel controls the gas flow through an impinger containing α-pinene, a heated column containing a methanol permeation tube, an impinger containing water, and air for dilution of the mixture. The airflow rates are controlled based on the

desired concentrations of α-pinene and methanol, and moisture content in combined gas stream. The methanol permeation tube (Metronics, M031979) emits methanol at a rate of 34620ng/min +/- 2% at 100 °C. Actual concentration of methanol can be calculated based on the methanol permeation rate and total airflow rate as described in equation 4:

$$C_{g,m} = \frac{r_m * 10^{-9} * RT}{V_{total} M_{c.m} P_{amb}} \quad (4)$$

where $C_{g,m}$ = methanol gas concentration (ppmv)

r_m = permeation rate of methanol tube (ng/min)

V_{total} = total airflow rate (mL/min)

P_{amb} = ambient pressure (Pa)

$M_{c.m}$ = molecular weight of methanol (g/mol)

R = universal gas constant (mL·Pa/mol·K)

T = temperature (K)

Four α-pinene impingers in series and four water impingers in series were used. The gas leaving the fourth impinger was saturated with either α-pinene or water. The temperature of the impinger was controlled to either 30 °C or 60 °C. The airflow through the water impinger was 120 mL/min. The airflow through the α-pinene impinger ranged from 11 to 13 mL/min. The vapor pressures and resulting concentrations of saturated vapor are shown in Table 4.

Table 4. Concentration calculation based on vapor pressure.

1 atm	α-pinene		water	
T (°C)	Vapor pressure (Pa)	Saturated conc. ppmv Equation (1)	Vapor pressure (Pa)	Saturated conc. ppmv Equation(1)
30	842	8311	4251	41952
60	3818	37680	19951	196906

The saturated concentration of contaminate gas, C_s (ppmv), was calculated according to equation 5:

$$C_s = \frac{10^6 * P_g}{P_{amb.}} \tag{5}$$

where

P_g = the vapor pressure of contaminant at the controlled temperature (Pa)

The contaminant gas concentration after dilution, $C_{g,ppm}$ (ppmv), was then calculated based on equation 6:

$$C_{g,ppm} = \frac{V_{i.}}{V_{total}} * C_s$$

$$V_{total} = V_{\alpha\text{-}p} + V_{methanol} + V_{dilution} + V_{water} \tag{6}$$

where

V_i = airflow rate through impinger where i is α-pinene and water (mL/min)

V_{total} = total airflow rate in the combined gas stream (mL/min)

Then, the unit of gas concentration was converted from ppmv to mol fraction using equation 7:

$$C_g = C_{g,ppm} * 10^{-6} \quad (7)$$

where

C_g = concentration of contaminant in gas (mole/mole)

Using the control panel, wet or dry gas containing a single or multiple contaminants can be generated to meet the experimental requirements. The laboratory equipment was capable of producing a concentration of methanol in air up to 1000 ppmv and α-pinene in air up to 8000 ppmv at total flowrates of 25 to 300 mL/min.

3.2.2.2 *Verification*

The weight loss of contaminant from the permeation tube or impingers were measured over a known time interval to verify the gas concentrations. The airflow rates through each impnger were also measured using a bubble meter. Then, the actual permeation rates, r_i' (ng/min), for methanol and α-pinene were calculated according to equation 8:

$$r_i' = \frac{W_c * 10^9}{t} \quad (8)$$

where

r_i' = actual permeation rate for contaminant gas where i is methanol or α-pinene (ng/min)

W_c = weight loss of contaminant (g)

t = total running time (min)

A comparison of generated gas concentrations based on vapor pressure and weight loss are shown in Table 5. It appears that the differences between these values are acceptable.

Table 5. Verification of methanol and α-pinene gas concentrations.

VOCs	W_c (g)	t (min)	Calculated permeation rate (ng/min)	Actual Permeation rate (ng/min)	Difference (%)
Methanol	0.14	3930	34620	35623	2.9
α-pinene	1.36	2920	472553	465753	1.5

3.2.3 Equilibrium in Impinger

An impinger was used to bring equilibrium between the contaminated gas and liquid into contact by bubbling the gas with known concentration through the RTIL continuously at 30 °C. Based on the emission data from dryers and presses at wood processing plants (Table 1), gas with a methanol concentration of 75 to 85 ppmv was used. The α-

pinene concentration in the gas was 250 to 300 ppmv. Equilibrium was reached when the liquid in impinger attained a constant concentration of the contaminants.

IL105 and 106 were used to determine the equilibrium time in an impinger due to their relatively higher viscosities. It took 24 hours or longer for both methanol and α-pinene to reach equilibrium in IL105 and 106 (Figure 9). Based on these results, an equilibrium time of 24 hours was used for our impinger absorption. Low concentration in the gas phase and the high concentration attained in the liquid phase resulted in a long equilibrium time. There was very little contaminant entering the impinger compared to the absorption capacity of the liquid.

After the equilibrium was reached between the two phases in the impinger, four identical liquid samples were taken from the impinger and placed in 4 ml vials. The sample size was 2 g. The vials were capped with a silicone septum to avoid gas leaking. The liquid samples were equilibrated at 30 °C in digital heatblock for 8 hours. When the equilibrium was reached between the two phases in vials, headspace analysis was done to determine contaminant concentration in the liquid.

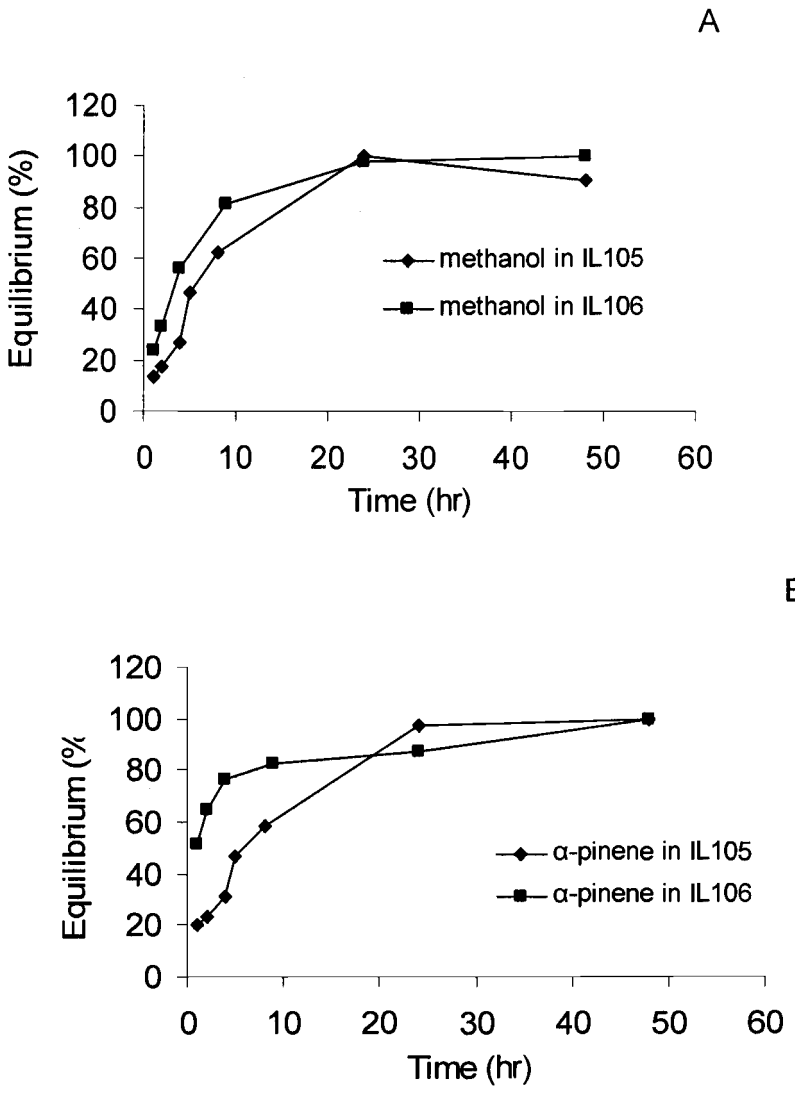

Figure 9. Equilibrium time for methanol (A) and α-pinene (B) absorbed continuously into IL105 and IL106 in impinger.

3.2.4 Headspace analysis on liquid samples

The contaminants in the ionic liquids were identified and quantified using headspace analysis by solid phase microextration (SPME). The principle of the technique is to establish equilibrium between liquid and gas phases, expose a SPME fiber to the gas phase for a fixed time period, then

desorb the fiber in the gas chromatograph (GC) and measure the response. The GC response is correlated to liquid concentration using liquids standards mixed gravimetrically.

3.2.4.1 SPME and GC-FID analysis

A SPME fiber coated with 75µm carboxen^{TM}-polydimethylsiloxane (PDMS) (Supelco, P325408) was used to sample headspace gas. The volatile organic compounds adsorbed onto fiber were identified and quantified by gas chromatography with a hydrogen flame ionization detector (GC-FID). A Shimadzu 2010 gas chromatograph was equipped with a Resteck Rtx-624 (94% dimethylpolysiloxane–6% cyanopropylphenyl) capillary column, 60 m in length, 0.53 mm internal diameter and 3 µm film thickness. The chromatographic elution was temperature programmed as follows: isothermal at 40 °C for 2 min, then from 40 to 60 °C at a rate of 5 °C /min, and to 220 at a rate of 50 °C /min, then isothermal hold at 220 °C for 5.8 min. The carrier gas was helium with a constant flow of 6.32 ml/min. The split/splitless injector was used in splitless mode and its temperature was maintained at 250 °C.

Compounds detected by the GC-FID are identified based on their unique retention times (RT). The area of a peak was calibrated to correspond to the concentration of compound in the liquid. The

chromatograph in Figure 10 shows the peaks and RT for methanol and α-pinene.

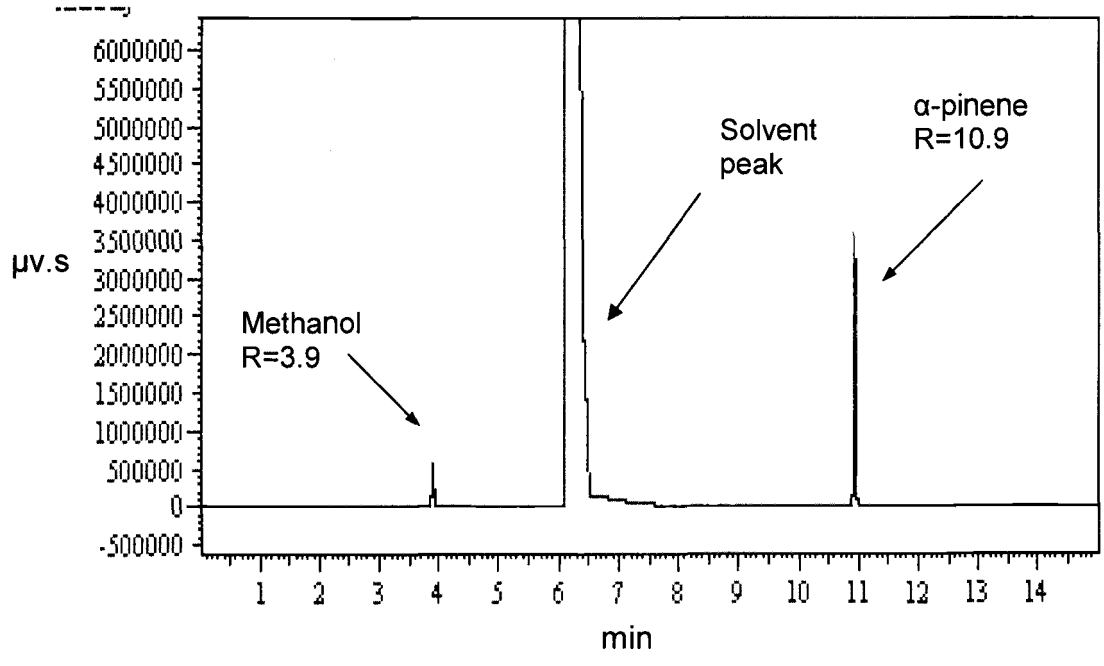

Figure 10. Typical GC-FID chromatographs for methanol and α-pinene

3.2.4.2 Calibration of headspace technique

Liquid standards with known concentrations were made as reference samples in order to quantify unknown liquid samples. All liquid standards were made based on mass by adding methanol and α-pinene into 2 g of RTIL. Three identical standards were made for each concentration. Four mL vials with silicone septa were used as sample containers. Concentrations were 0 ppmw, 20, 50, 100 and 200 ppmw for both methanol and α-pinene. The unit was converted from ppmw to mol fraction

based on equation 9. The standards were thoroughly mixed prior to equilibrium.

$$C_{L.S} = 10^{-6} * C_{L,ppm} * M_S / M_C \quad (9)$$

where

$C_{L.S}$ = concentration of contaminant in liquid standards (mol/mol)

$C_{L,ppm}$ = concentration of contaminant in liquid (ppmw)

M_S = molecular weight of solvent (g/mole)

M_C = molecular weight of contaminant (g/mole)

The liquid standards and liquid samples from the impinger were equilibrated at 30 °C in a heatblock for 8 hours. The SPME fiber was then put into the vial headspace for 20 minute to adsorb contaminants. The fiber was then immediately thermally desorbed in the injector of the GC for 5 minutes at 230 °C.

The calibration curves for the headspace technique were created from the standards. These curves were used to determine the concentrations in the impinger samples. Figure 11 shows example of these curves for RTIL HMIM-PF_6.

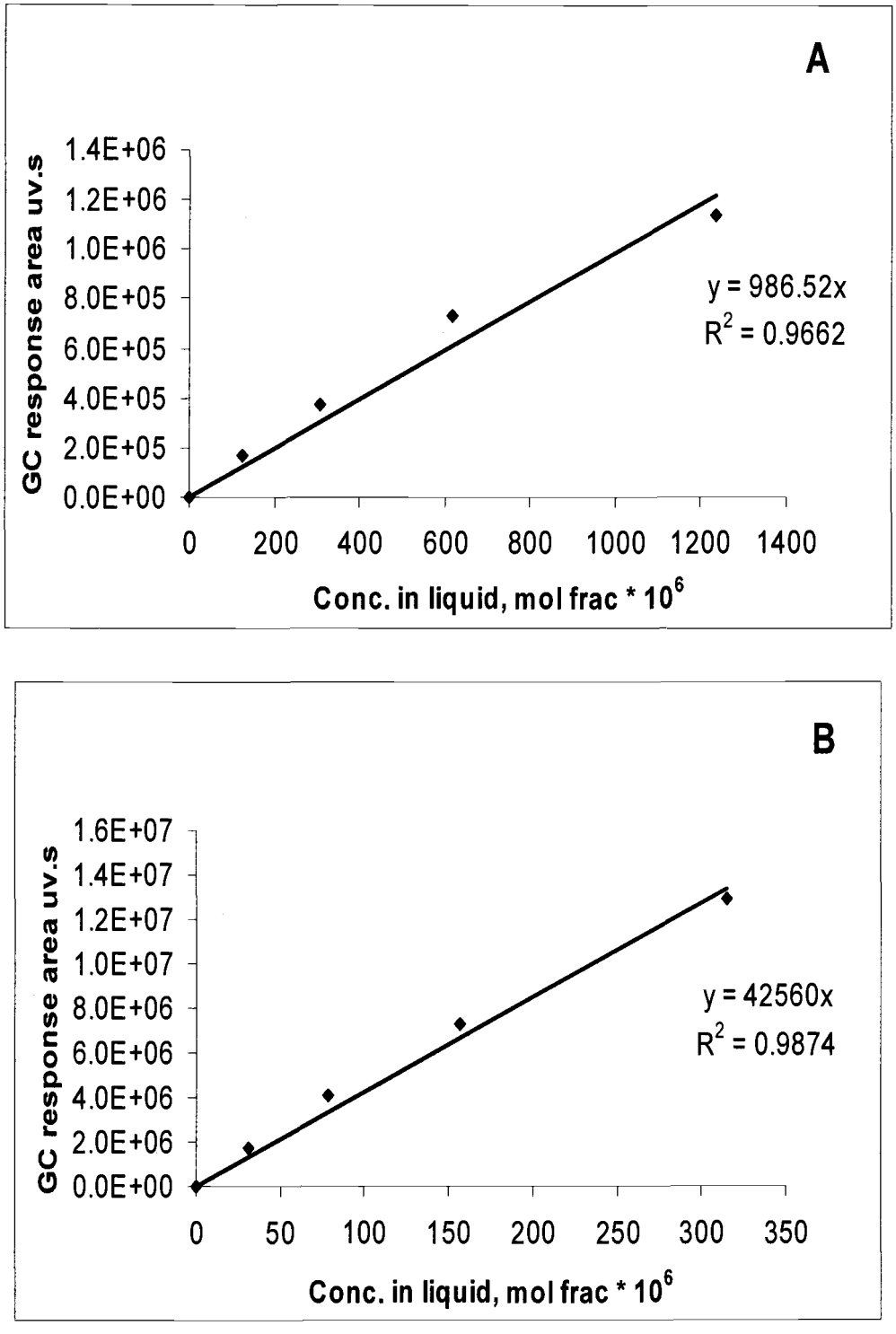

Figure 11. SPME calibration curves for methanol (A) and α-pinene (B) in RTIL HMIM-PF_6

The slopes of these curves are termed as response factors (*RF*). The contaminant concentration in liquid samples from impinger was then determined by equation 10:

$$C_L = \frac{A}{RF} \tag{10}$$

where

A = GC peak area corresponded to gas sample injected (μv·s)

RF = the slopes of calibration curves (μv·s/ng)

3.2.5 Calculation of Henry' constants

As mentioned in literature review, Henry' constants (H) can be dimensionless and were calculated based on the equilibrium between the two phases in impinger using the equation 11:

$$H = \frac{C_g}{C_L} \tag{11}$$

C_g = concentration of contaminate in gas (mole/mole)

C_L = concentration of contaminate in liquid (mole/mole)

3.3 Phosphonium-based RTILs

3.3.1 Overview of experimental procedures

The experimental procedure for determining Henry's constants for the methanol and α-pinene in phosphonium-based RTILs is shown in Figure 12. The general procedure is to prepare liquid samples containing a known concentration of contaminate. A small amount of the mixture is placed in a vial. After the equilibrium is reached between gas phase and liquid phase, the contaminant concentration in the headspace is determined. Detailed information for these procedures is described in the following sections.

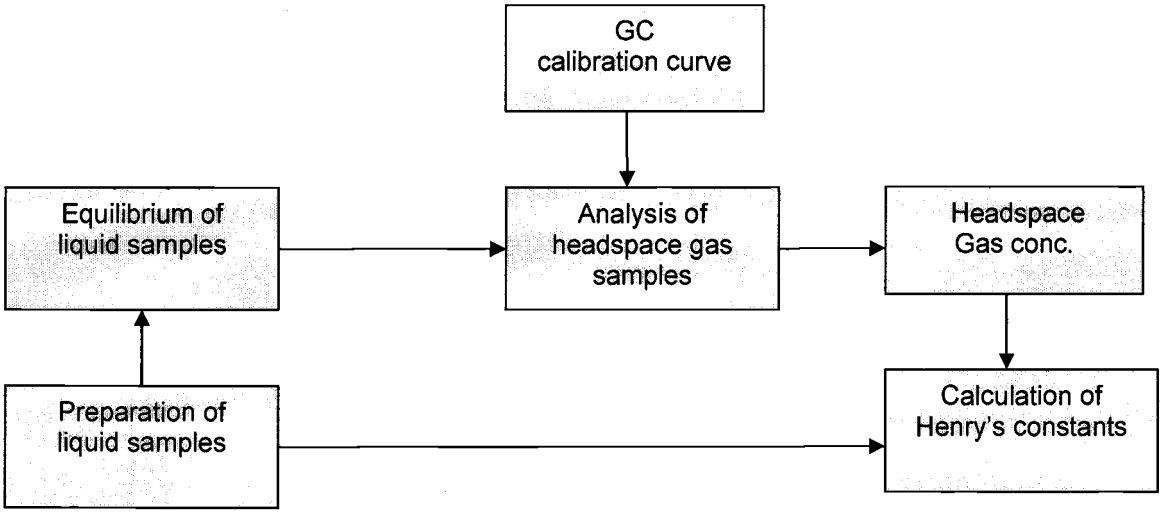

Figure 12. Experimental procedures for determining Henry's constants for contaminates in phosphonium-based RTILs.

3.3.2 Preparation of liquid samples

Samples of each RTIL were made containing methanol, α-pinene and water, singly or mixed. The concentrations of methanol and α-pinene in the RTILs were based on both the preliminary test and contaminant gas concentration from wood plant. The headspace gas concentration over these liquid samples would be similar to the values in Table 1. For example, the liquid samples made for RTIL105 are listed in Table 6. The concentration for the other RTILs are provided in the Appendix.

Table 6. Concentration of methanol and α-pinene in IL105.

Temp. (°C)	Methanol		α-pinene		Mix of methanol and α-pinene	
	Conc. (ppmw)		Conc. (ppmw)		Conc. methanol/α-pinene (ppmw)	
	Dry	Wet	Dry	Wet	Dry	Wet
30	97	---	3750	---	97/3750	---
60	29	29	1125	1125	29/1125	29/1125
90	8	---	375	---	8/375	8/375

The liquid samples for the other three RTILs, TBPD, THPD and 106 were similar. Four replicate samples were made for each condition. The sample size was 0.82 g. The samples were stored in 4 mL vials which were capped with septa to avoid any escape of gas vapor. 2% moisture

content based on the mass of RTILs was used as wet condition in this study.

3.3.3 Equilibrium of liquid samples

A rotating vial holder was used to promote the complete mixing between methanol, α-pinene, water, and the RTILs. After complete mixing, the liquid samples in 4 ml vials were equilibrated in a heatblock for 8 hours so that the contaminants could reach equilibrium between the gas and liquid phases. The equilibrium temperatures included 30 °C, 60 °C, and 90 °C based on the experimental design in Section 3.3.2. During equilibrium, some of contaminants entered the gas phase from the liquid phase.

3.3.4 Analysis of headspace gas samples

The identification and quantification of contaminants in the headspace over ionic liquids were done using direct gas injection. The principle of the technique was to establish equilibrium between liquid and gas phases, then inject a gas sample from the headspace into the gas chromatograph (GC) to determine the mass of contaminant in the injection. The mass in the headspace was then obtained based on a ratio of the injection volume to headspace volume.

3.3.4.1 Sampling of headspace gas

When the samples reached equilibrium in the heatblock, 0.2 mL headspace gas above liquid phase was sampled with 1 mL gas-tight syringe and then injected into the GC immediately. At room temperature, the syringe was flushed through pumping air ten times to clean the condensed contaminant on syringe surface before next injection. The operating parameters for the GC are described in Section 3.2.4.1.

3.3.4.2 GC calibration curve

The masses of methanol and α-pinene injected into GC were correlated to GC peak area and concentration of liquid standards. The standards contained methanol and α-pinene in CH_2Cl_2, each at concentrations of 0 mg/L, 4, 40, and 400 mg/L for both methanol and α-pinene. A 5.0 µL syringe was used to inject 1 µL of sample. The plots of GC peak area (µv·s) as function of mass (ng) of methanol or α-pinene were used as calibration curves (Figure 13).

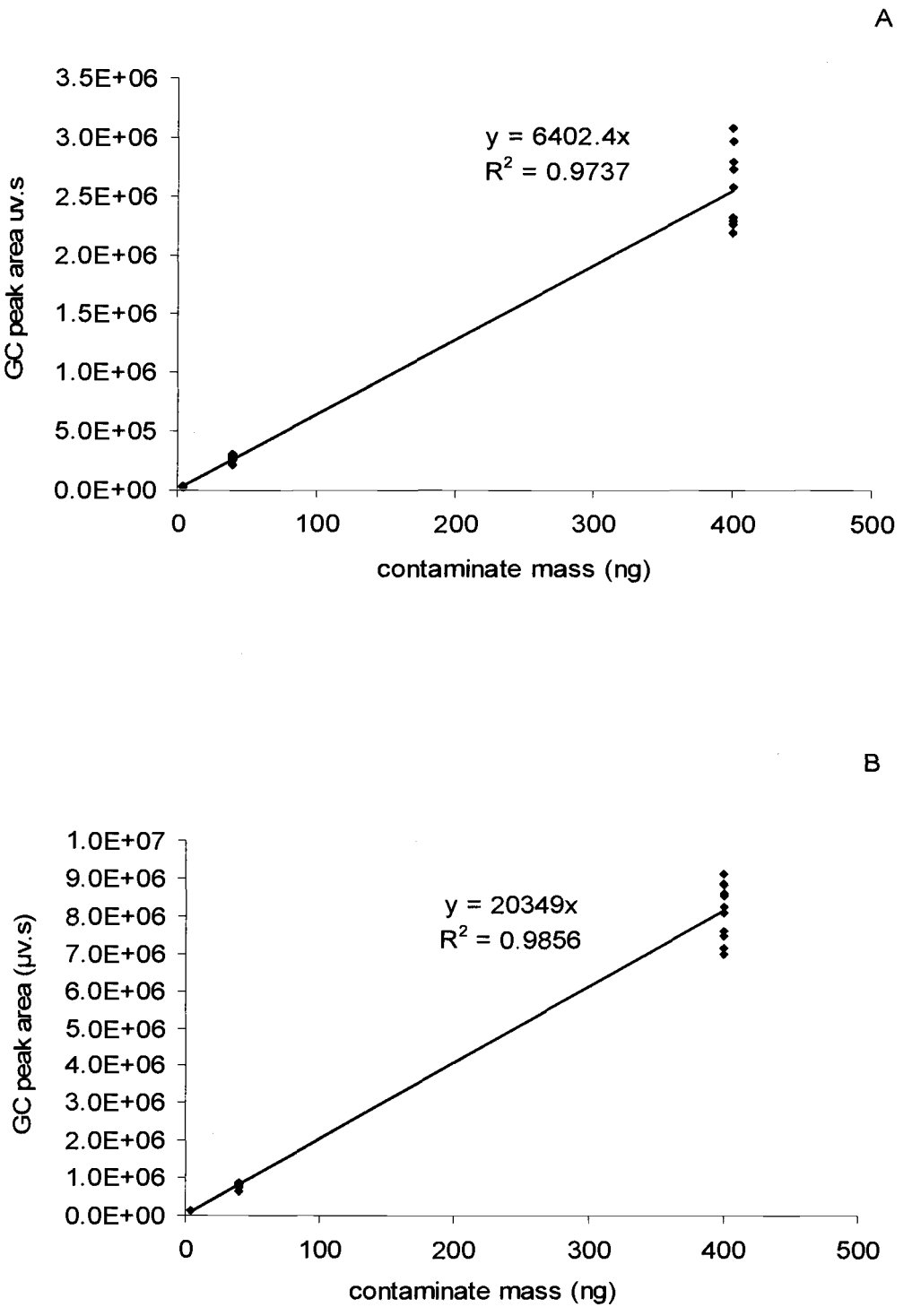

Figure 13. GC calibration curves for methanol (A) and α-pinene (B).

Liquid standards were injected before and after injections of gas samples on each day to check the stability of the GC. The variabilities of RF for methanol and α-pinene standards checked daily are plotted as function of date in Figure 14.

The RF during the experiments varied ± 20% for methanol and ± 12% for α-pinene.

3.3.4.3 Evaluation of sampling method

Henry's constants of contaminants in RTILs were measured at 30 °C, 60 °C and 90 °C respectively. However, the gas-tight syringe was always at room temperature (25 °C). This temperature difference between the gas samples and the syringe may lead to gas condensation or adsorption onto the surface of syringe. A procedure to verify this was developed.

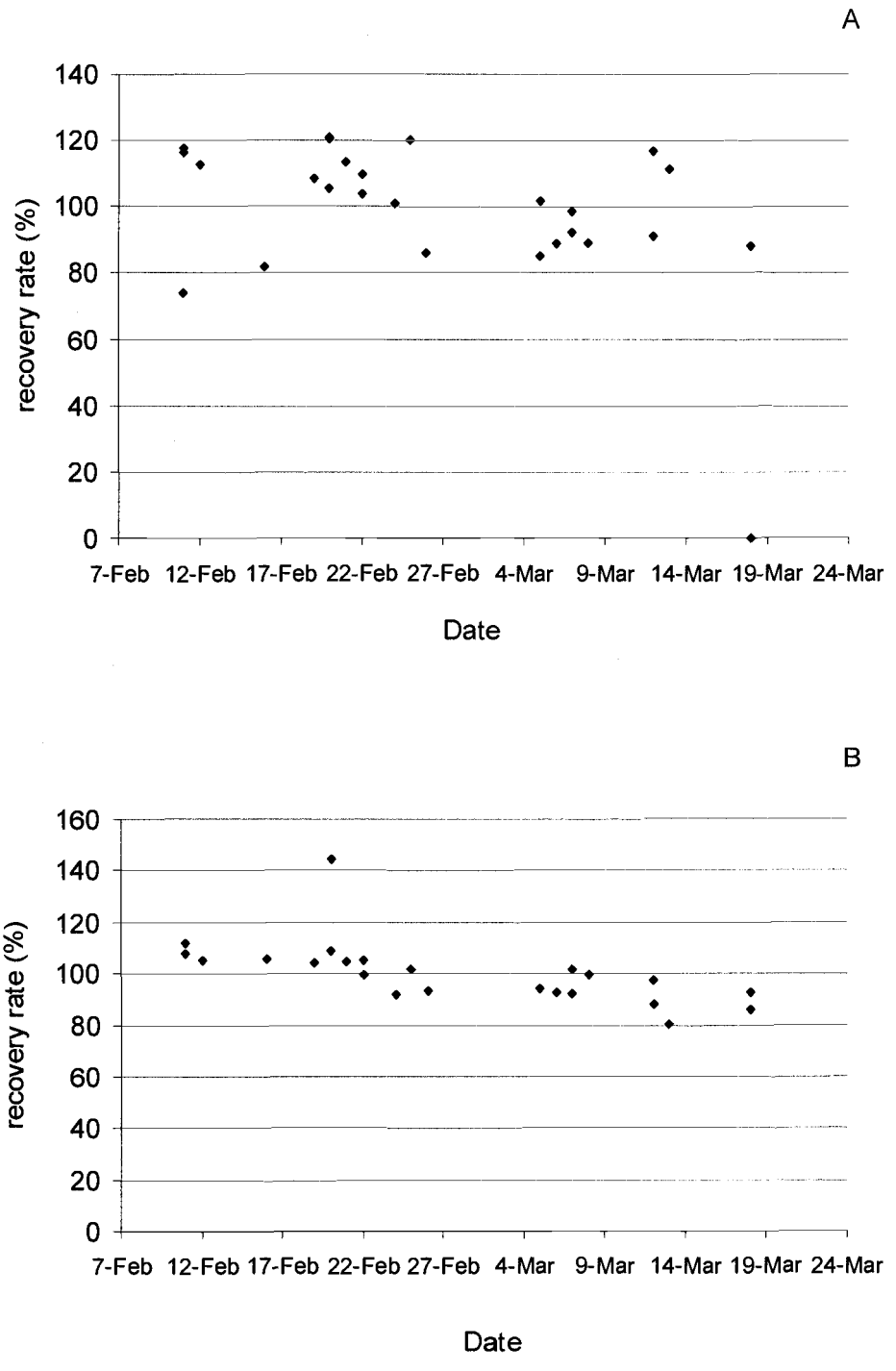

Figure 14. The variability of RF for GC calibration curve: (A) methanol and (B) α-pinene.

Gas containing a known concentration contaminant ($C_{g,known}$) was generated measured at 30 °C, 60 °C, and 90 °C as described in Section 3.2.2. 0.2 mL of this gas was sampled using the gas-tight syringe for each injection and then injected into the GC immediately. The gas concentration ($C_{g,ppm}$') in the syringe after condensation was then determined based on the equation 12:

$$C_{g,ppm}' = \frac{10^{-9} A / (RF * M_c) * RT}{0.0002L * P_{amb.}} * 10^6 \quad (12)$$

where

$C_{g,ppm}$' = contaminant concentration in gas phase (ppmv)

A = GC peak area corresponded to gas sample injected (μv·s)

RF = the slopes of calibration curves (μv·s/ng)

0.0002 L = gas sample size injected

This concentration is compared to the concentration at which the gas was made in Table 7. The recovery rate of α-pinene was up to 99%, so the loss during syringe transfer could be negligible. The recovery rate of methanol was even over 100%, which might be caused by residual contaminate in syringe. Therefore, the loss of contaminates on syringe surface is not a big concern in this study.

Table 7. Data for calculating condensation of contaminates on syringe surface.

Gas T	Methanol			α-pinene		
(°C)	$C_{g,known}$	$C_{g,ppm}$'	Recovery rate (%)	$C_{g,known}$	$C_{g,ppm}$'	Recovery rate (%)
30	72	81	112	234	227	97
30	72	81	112	234	229	98
60	71	72	101	234	231	99
60	71	73	103	234	233	100
90	73	75	102	234	229	98
90	73	75	102	234	238	102
Ave.	72	76	105	234	231	99

3.3.4.4 Measurement of headspace gas concentration, C_g

Figure 13 was used to determine the concentration mass injected in the 0.2 mL gas sample. Equation 13 was then used to determine the concentration of methanol and α-pinene in the headspace.

$$C_g = \frac{10^{-9} A / (RF * M_C) * RT}{0.0002L * P_{amb.}} \quad (13)$$

Where

C_g = contaminant concentration in gas phase (mole/mole)

0.0002 L = gas sample size injected

3.3.4.5 Determination of liquid concentration, C_L

The final contaminant concentration in liquid (C_L) is lower than the initial concentration (C_{Li}) because some contaminant entered headspace gas phase after equilibrium. C_L was calculated using equation 14:

$$C_L = \frac{\left[C_{L,i} * m_{IL} - 10^{-9} A / (RF * 0.2mL)(4.84mL - 0.82g/e_s)\right]}{m_{IL}} * \frac{M_s}{M_c} \qquad (14)$$

where

C_L = contaminant concentration in liquid (mole/mole)

C_{Li} = initial concentration liquid (g/g)

m_{IL} = mass of ionic liquid for each liquid sample (g)

e_S = density of ionic liquid (g/mL)

0.2 mL= gas sample size injected

4.84 mL= is the volume of 4mL vial contained sample

0.82g = the mass of liquid sample

3.3.5 Calculation of Henry' constants

Henry' constants were determined for both methanol and α-pinene in each RTIL tested though dividing C_g by C_L based on the equation (11) in Section 3.2.5.

3.4 Equilibrium in impinger

An impinger was used to bring equilibrium between the contaminated gas and liquid by bubbling the gas through the RTIL continuously. The gas stream including methanol gas of 70~80ppmv (part per million based on volume) and α-pinene gas of 260~290 ppmv, were bubbled continuously through the impingers containing TBPD and THPD at 60 °C with and without moisture in the gas stream. The moisture content in air stream was set at 20% relative humidity (RH).

After the equilibrium was reached between the two phases in the impinger, four identical 0.82 g liquid samples were taken from the impinger and stored in 4ml vials. The vials were capped with a silicone septum to avoid gas leaking. The liquid samples were equilibrated at 60 °C in heatblock for 8 hours. When the equilibrium was reached between the two phases in vials, headspace analysis was done to determine contaminant concentration in the liquid.

Then, Henry's constants for contaminants in each RTIL were calculated using equation (11).

All data from both vial and impinger samples were analyzed by a student T-test using a 95% confidence level. Comparison was made between the Henry's constants among the temperature, between the dry and wet conditions and among the RTILs.

3.5 Desorption of contaminates from RTILs

Because the RTILs are viscous, low vacuum and high temperature were used to remove contaminants from used RTILs. Rotaevaporator was used to increase evaporating surface and an oil bath was used to control recycling temperature. The removal efficiency was measured at 30 °C, 70°C and 90 °C under 176 torr. In addition, low pressure of 0.5 mtorr was applied to remove contaminant at 30 °C. The time interval for each sample was two hours.

Chapter 4 Results and Discussion

4.1 Imidazolium-based RTILs

4.1.1 Henry's constant for methanol and α-pinene in imidazolium-based RTILs

4.1.1.1 Preliminary test

Liquid samples with 0.01 wt% methanol in RTILs BMIN-BF_4N_2, BMIN-PF_6, HMIN-PF_6, or OMIN-PF_6 were prepared. The headspace gas was sampled with SPME fiber and desorbed in GC as described in Section 3.2.4. Methanol gas concentration in headspace is proportional to the GC peak area and GC responses are shown in Figure 17 in increasing order.

Henry's constant should be related to peak area. Figure 15 suggested that increasing the length of chain on cations increased Henry's constant and that anion [$BF_4N_2^-$] results in a lower Henry's constant than anion [PF_6^-].

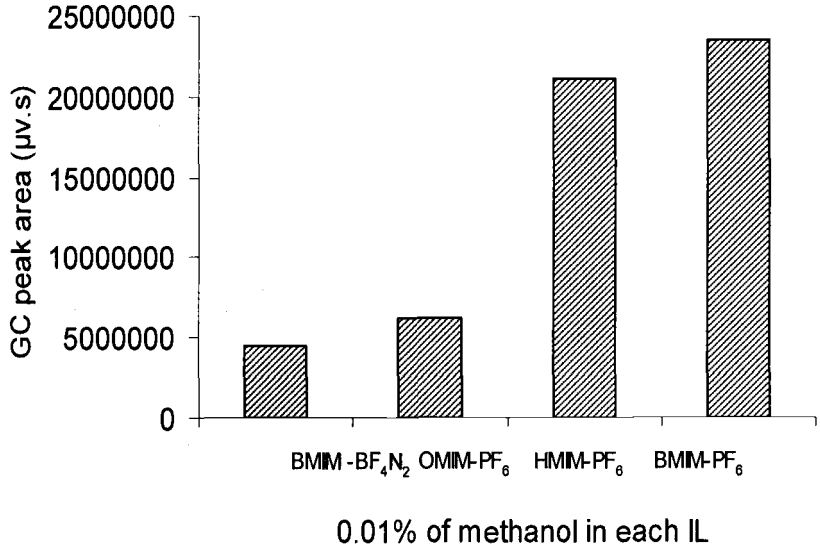

Figure 15. Headspace gas concentration responded as GC peak area for methanol in RTILs BMIN-BF_4N_2, BMIN-PF_6, HMIN-PF_6, or OMIN-PF_6.

4.1.1.2 Henry's constant

Henry's constants for methanol and α-pinene in BMIN-PF_6, HMIN-PF_6 and OMIN-PF_6 were determined using SPME and GC-FID technique (Table 8). The results for methanol agreed with the preliminary test (Figure 15). The Henry's constants for methanol and α-pinene decreased with increasing the length of chain on cations.

Table 8. Henry's constants (mol fraction) of methanol and α-pinene in imidazolium-based RTILs at 30 °C.

VOCs	OMIN-PF_6	HMIN-PF_6	BMIN-PF_6
methanol	0.007	0.01	0.62
α-pinene	0.0004	0.001	0.002

4.1.2 Issues associated with SPME and GC-FID technique

The adsorption properties of the SPME fiber were found to change with time due to the weariness of fiber. This changes the equilibrium between contaminant absorbed on fiber and contaminated gas concentration. Therefore, SPME fiber should be calibrated frequently.

In addition, the equilibrium of a single component on the SPME fiber was changed when multiple components were adsorbed. This made determining a calibration curve for SPME quite complicated. Therefore, new sampling technique was developed.

4.1.3 Issues associated with imidazolium-based RTILs

Some negative issues came up with the imidazolium-based ILs with anion [PF_6^-] during experiment. First, results were not reproducible. Second, color changed from light yellow to brown or dark when temperature was up to 90 °C. Third, a white gas was generated from the sample. It was speculated that the gas was HF. Deterioration of glassware also suggested the presence of this compound. The difficulty in reproducing results is explained by the HF breaking down the methanol and α-pinene.

Because of these difficulties with the imidazolium-based ILs, phosphonium-based RTILs were selected for the further experiments

4.2 Phosphonium-based RTILs

4.2.1 Effects of temperature and multiple contaminants on the Henry's constants

The Henry's constants for methanol and α-pinene in RTIL105, TBPD, THPD and RTIL106 are shown in Figure 16, 17, 18 and 19. As expected, the Henry's constants increased as temperature increased for both methanol and α-pinene in all four RTILs. Temperature has a strong effect on Henry's constant. These increases were nonlinear and Henry's constant increased by a factor of 8 to 10 as temperature increased from 30 °C to 90 °C. Low temperature is preferable for an absorption system to remove VOCs from the exhaust gas.

According to the temperature dependence of Henry's constant described in equation 3, A_{H_i} and B_{H_i} as constants for each solute–absorbent combination were determined by linear regression between ln(H_i) and $1/T$. The plots of ln(H_i) versus $1/T$ for methanol and α-pinene with IL105, TBPD, THPD and 106 are shown in Figure 16, 17, 18 and 19 respectively. The values of A_{H_i} and B_{H_i} obtained from these regression curves are listed in Table 9. The experimental data fits Equation 3 very well. The regression coefficients varied from 0.99 to 1 except for methanol, α-pinene in RTIL106. This is discussed further in Section 4.2.1.4.

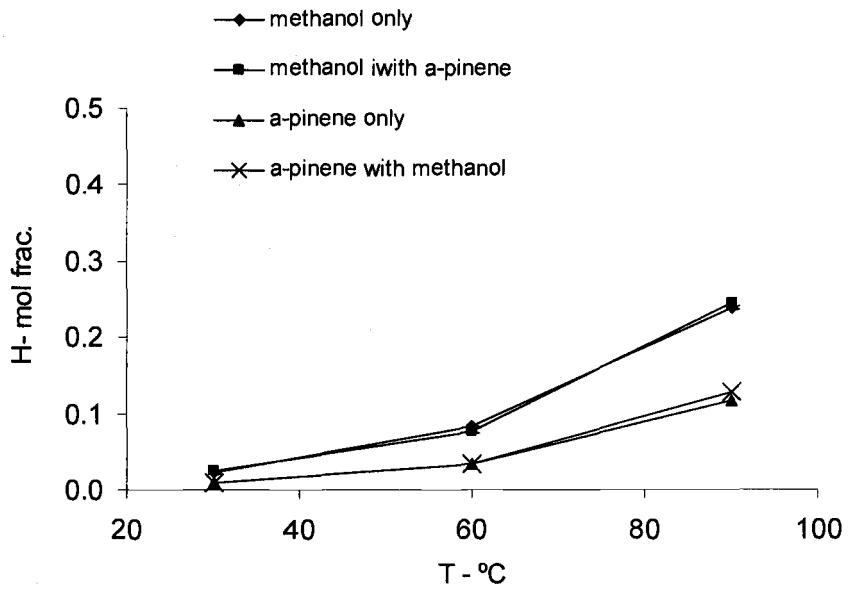

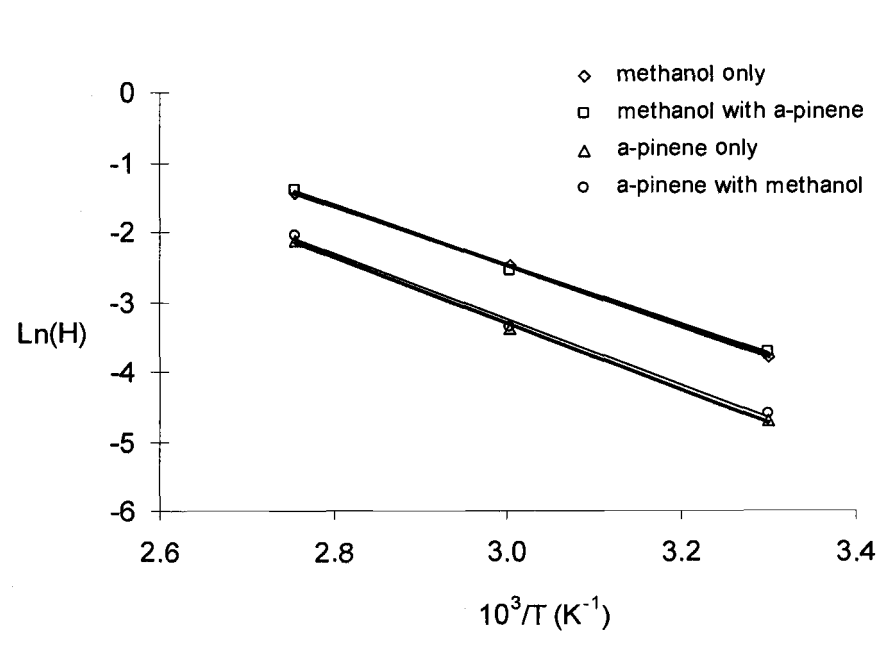

Figure 16. Henry's constant versus temperature (A) and natural log vs. reciprocal absolute temperature (B) for IL105. Methanol with α-pinene or a-pinene with methanol indicates a small amount of the second contaminant is present. Each point is the mean of 3 data points.

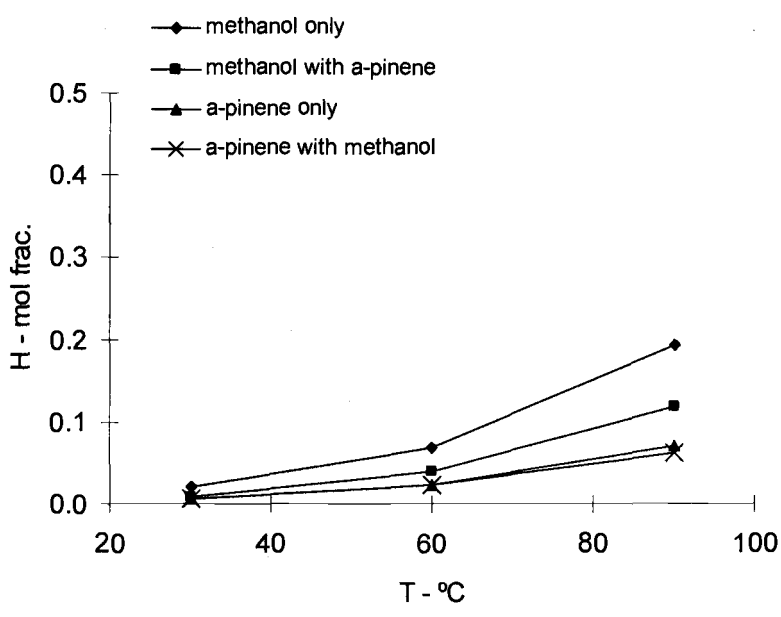

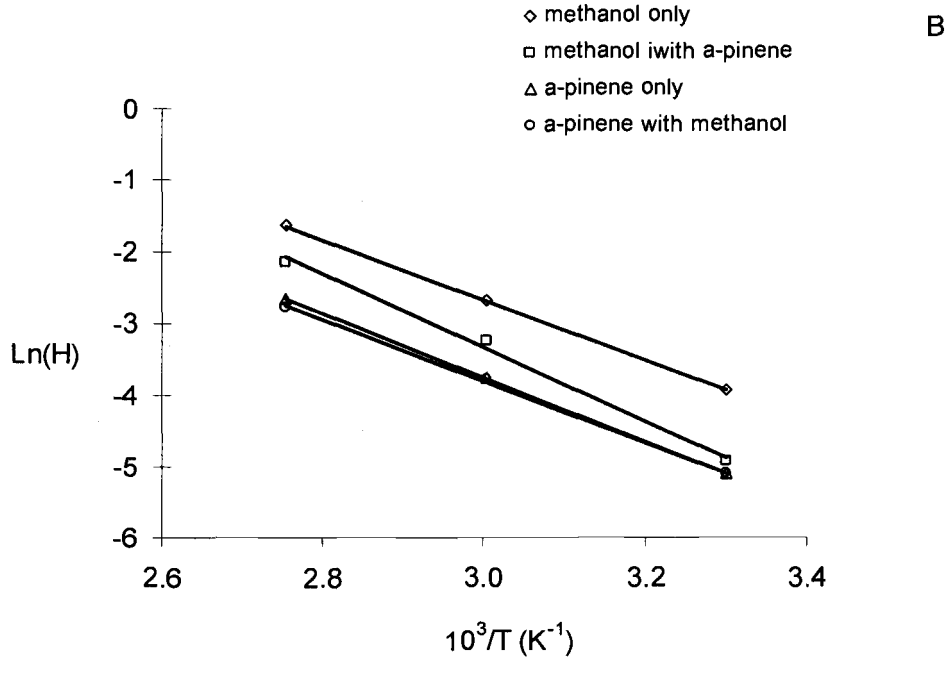

Figure 17. Henry's constant versus temperature (A) and natural log vs. reciprocal absolute temperature (B) for TBPD. Methanol with α-pinene or a-pinene with methanol indicates a small amount of the second contaminant is present. Each point is the mean of 3 data points.

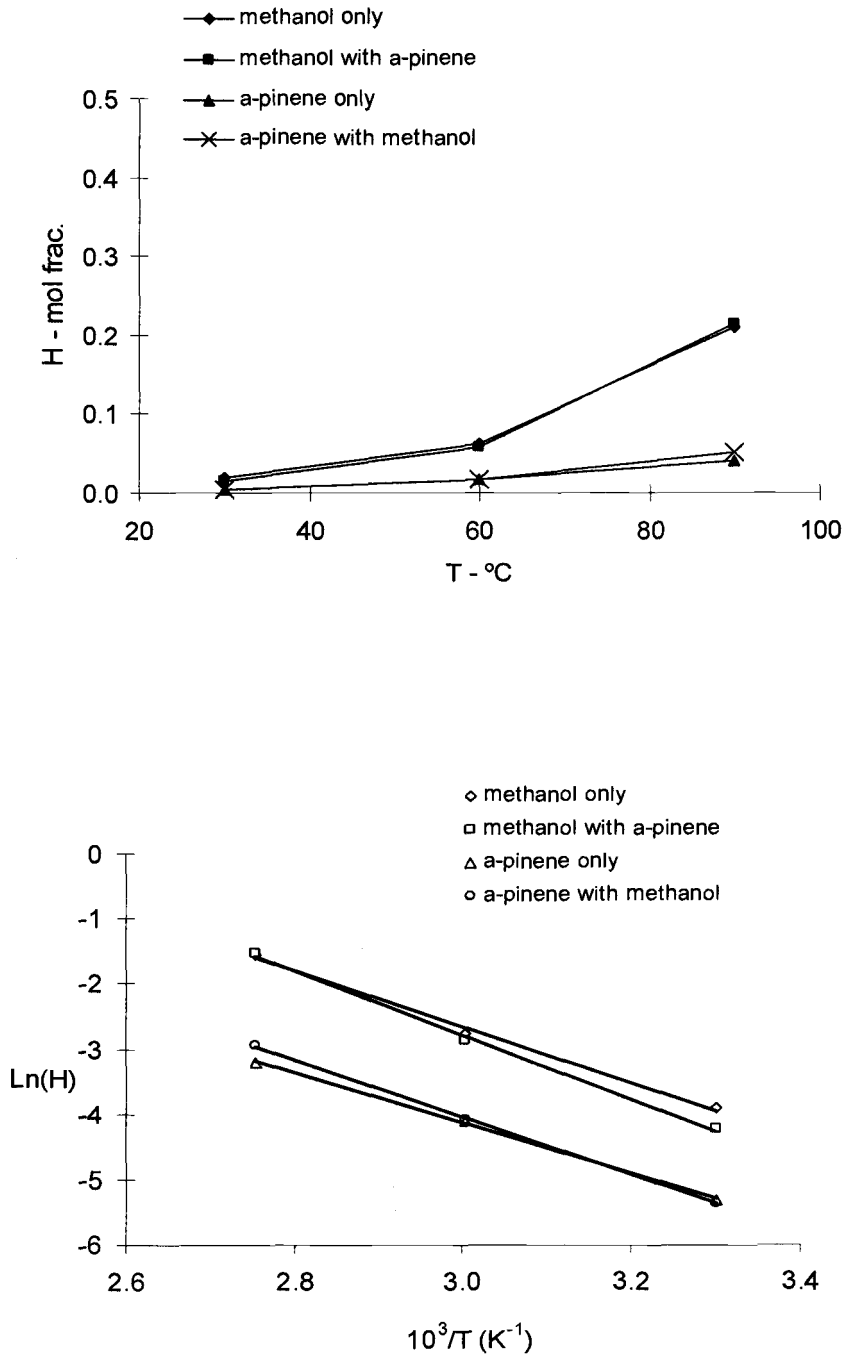

Figure 18. Henry's constant versus temperature (A) and natural log vs. reciprocal absolute temperature (B) for THPD. Methanol with α-pinene or a-pinene with methanol indicates a small amount of the second contaminant is present. Each point is the mean of 3 data points.

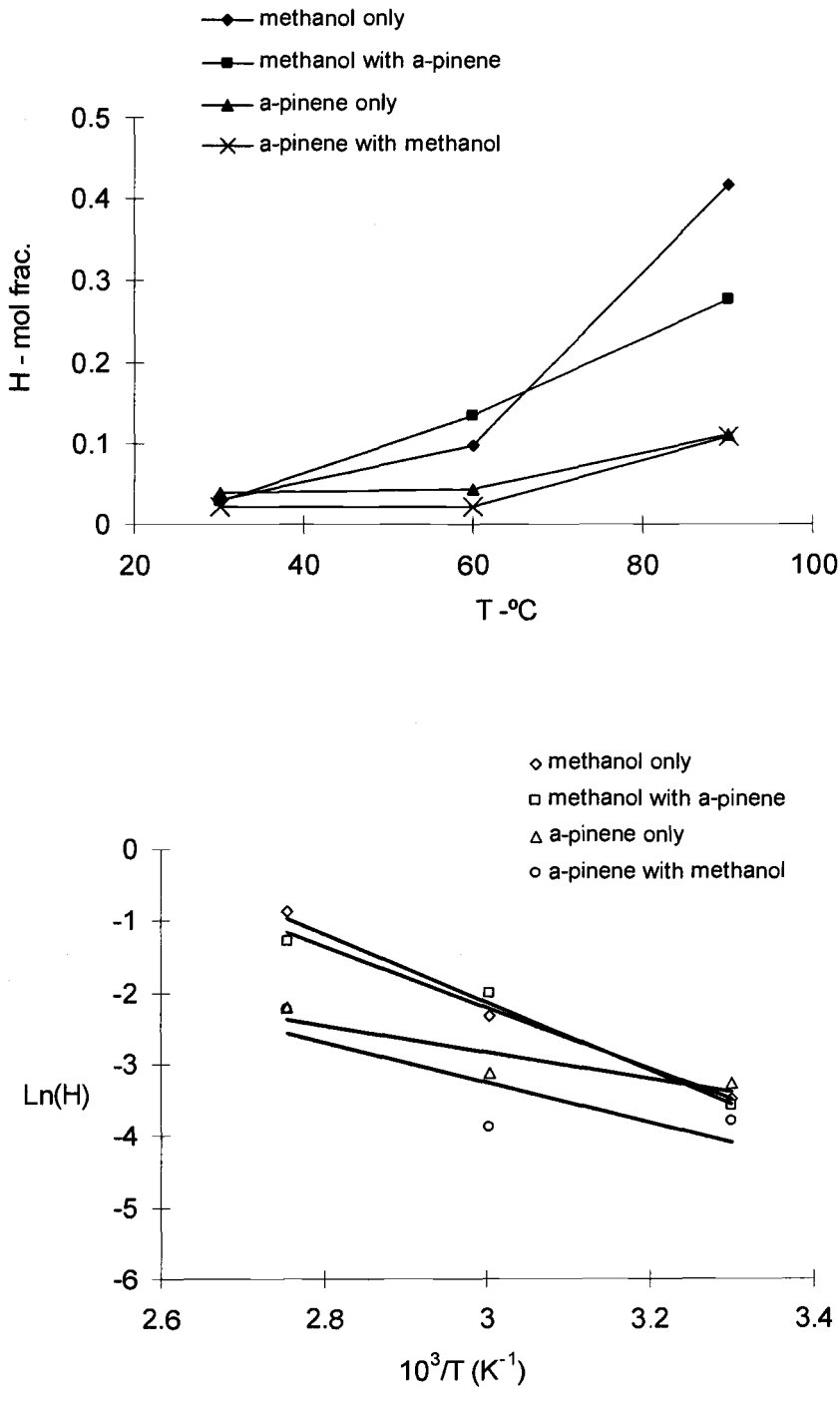

Figure 19. Henry's constant versus temperature (A) and natural log vs. reciprocal absolute temperature (B) for IL106. Methanol with α-pinene or a-pinene with methanol indicates a small amount of the second contaminant is present. Each point is the mean of 3 data points.

Table 9. Values of A_{H_i} and B_{H_i} for equation 10 (methanol alone or α-pinene alone as contaminant).

VOCs	RTIL105			TBPD			THPD			RTIL106		
	A_{H_i}	B_{H_i}	R^2	A_{H_i}	B_{H_i}	R^2	A_{H_i}	B_{H_i}	R^2	A_{H_i}	B_{H_i}	R^2
Methanol	10.26	-4.25	1.00	9.82	-4.16	1.00	10.26	-4.31	0.995	12.08	-4.74	0.98
α-pinene	10.76	-4.70	1.00	9.72	-4.49	1.00	7.59	-3.91	1.00	2.78	-1.87	0.81

4.2.1.1 RTIL105

No significant change in Henry's constant was observed for methanol when α-pinene was present compared to when methanol was the only contaminant (p=0.1, 0.06 and 0.08 for methanol at 30 °C, 60 °C and 90 °C respectively, Table 10 and Figure 16). Similarly, no significant change in Henry's constant was observed for α-pinene when methanol was present compared to when α-pinene was the only contaminant (p=0.14, 0.92 and 0.15 for α-pinene at 30 °C, 60 °C and 90 °C respectively, Table 10 and Figure 16).

Table 10. Henry's constants (mol fraction) under dry condition for methanol and α-pinene in RTIL105.

T (°C)		methanol		α-pinene	
		alone	with α-pinene	alone	with methanol
30	mean	0.0224	0.0241	0.0091	0.0100
	stdev	0.0009	0.0011	0.0001	0.0008
60	mean	0.0828	0.0772	0.0340	0.0341
	stdev	0.0011	0.0027	0.0012	0.0010
90	mean	0.2384	0.2461	0.1182	0.1287
	stdev	0.0024	0.0039	0.0092	0.0046

It indicates that the effects of multiple contaminants on the solubility of individual contaminant into IL105 are negligible. This result is expected at low concentrations. Also, methanol is a small, polar molecule, while α-

pinene is larger, unpolar molecule. They would form different types of bonding with ILs, then they shouldn't interfere each other too much.

4.2.1.2 TBPD

Henry's constant for methanol decreased significantly when α-pinene was present compared to when methanol was the only contaminant (p=0.00 at each, 30 °C, 60 °C and 90 °C, Table 11 and Figure 17). No significant change in Henry's constant was observed for α-pinene when methanol was present compared to when α-pinene was the only contaminant at 30 °C and 60 °C, while Henry's constant decreased significantly at 90 °C (p=0.47, 0.92 and 0.00 for at 30 °C, 60 °C and 90 °C respectively, Table 11 and Figure 17).

Table 11. Henry's constants (mol fraction) under dry condition for methanol and α-pinene in TBPD.

T		methanol		α-pinene	
(°C)		alone	with α-pinene	alone	with methanol
30	mean	0.0199	0.0073	0.0061	0.0060
	stdev	0.0000	0.0002	0.0002	0.0002
60	mean	0.0682	0.0393	0.0232	0.0230
	stdev	0.0043	0.0018	0.0006	0.0003
90	mean	0.1932	0.1181	0.0709	0.0622
	stdev	0.0068	0.0047	0.0020	0.0006

It appears that the presence of multiple contaminants didn't increase the Henry's constant for methanol and α-pinene in TBPD and even decreased the Henry's constant of methanol in TBPD at all three temperatures. The Henry's constant for α-pinene decreased in TBPD at 90 °C.

4.2.1.3 THPD

Henry's constant for methanol decreased significantly when α-pinene was present compared to when methanol was the only contaminant (p=0.00, at each, 30 °C, 60 °C and 90 °C, Table 12 and Figure 18). However, in a practical sense, theses differences are unlikely to impact an absorption process. No significant change in Henry's constant was observed for α-pinene when methanol was present compared to when α-pinene was the only contaminant from 30 °C to 60 °C, while Henry's constant increased significantly at 90 °C (p=0.33, 0.52 and 0.01 for at 30 °C, 60 °C and 90 °C respectively, Table 12 and Figure 18).

It indicates that the presence of multiple contaminants did increase the solubility of methanol in THPD from 30 °C to 90 °C and decreased the solubility of α-pinene in THPD at higher temperature, 90 °C.

Table 12. Henry's constants (mol fraction) under dry condition for methanol and α-pinene in THPD.

T (°C)		methanol		α-pinene	
		alone	with α-pinene	alone	with methanol
30	mean	0.0200	0.0145	0.0049	0.0047
	stdev	0.0005	0.0005	0.0000	0.0006
60	mean	0.0629	0.0569	0.0165	0.0168
	stdev	0.0009	0.0000	0.0005	0.0004
90	mean	0.2111	0.2152	0.0409	0.0523
	stdev	0.0008	0.0223	0.0006	0.0045

Compared to IL105, both TBPD and THPD had Henry's constants that were more favorable for absorption. TBPD and THPD have the same anion, dodecylbenzenesulfonate; whereas IL105 has dicyanamide. IL105 and THPD have the same cation, trihexyltetradecylphosphonium. Therefore, it appeares that the dodecylbenzenesulfonate anion has a stronger interaction with both methanol and α-pinene than the dicyanamide anion.

4.2.1.4 RTIL106

The linear regression of $1/T$ and $\ln(H_i)$ for the α-pinene in IL106 didn't fit the data as well as the other three ILs (Figure 19). Some error might have occurred either during sample preparation or sample analysis

in GC. Henry's constant for α-pinene at 60 °C is close to that at 30 °C for both α-pinene alone and with methanol (Table 13 and Figure 19). It appeares that the actual concentration of the liquid samples were lower than used concentration in calculation, which indicates that error occurred during sample preparation. Therefore, the data for combination of α-pinene and IL106 at 60 °C are not reliable.

Table 13. Henry's constants (mol fraction) under dry condition for methanol and α-pinene in RTIL106.

T		methanol		α-pinene	
(°C)		alone	with α-pinene	alone	with methanol
30	mean	0.0310	0.0278	0.0385	0.0225
	stdev	0.0029	0.0005	0.0013	0.0130
60	mean	0.0971	0.1348	0.0441	0.0206
	stdev	0.0023	0.0096	0.0003	0.0021
90	mean	0.4174	0.2774	0.1096	0.1090
	stdev	0.0030	0.0132	0.0020	0.0115

4.2.2 Comparison of Henry' constants among IL105, TBPD, THPD and IL106.

4.2.2.1 Methanol

Henry' constants for methanol in the four RTILs are compared in Figure 20.

A

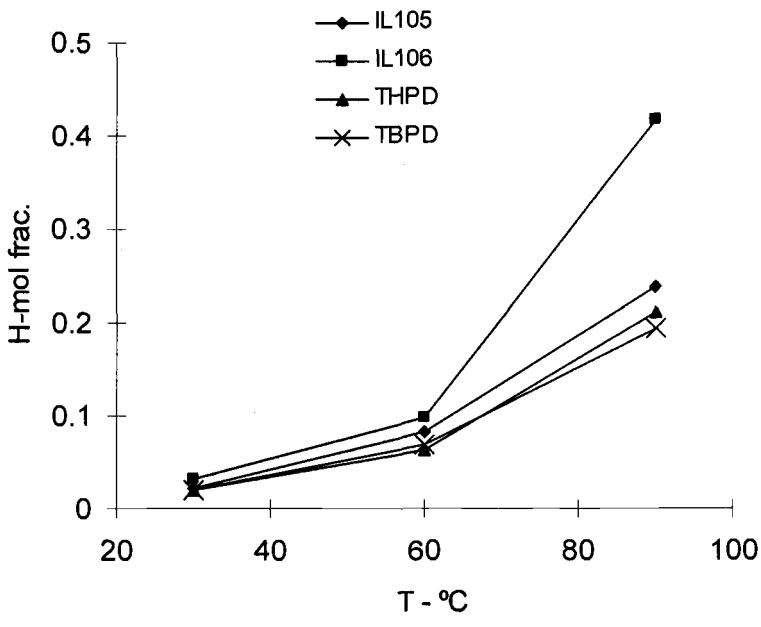

B

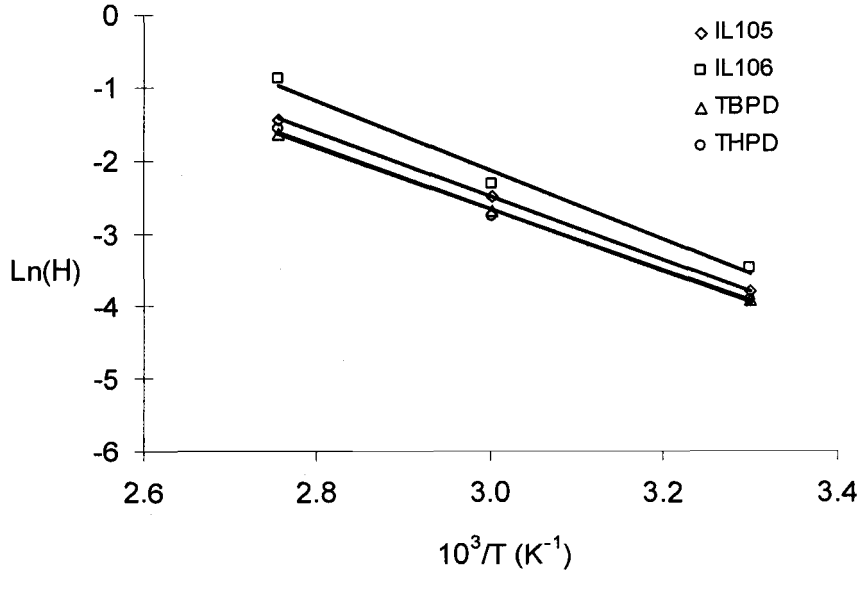

Figure 20. Henry's constant versus temperature (A) and natural log vs. reciprocal absolute temperature (B) for methanol in four ILs (Data from methanol alone as contaminant: two-component system). Each point is the mean of three data points.

For TBPD and THPD, the Henry's constants for methanol were not statistically different at 30°C and 60°C (p=0.92 at 30°C and p=0.11 at 60°C, Figure 20). However, the Henry's constant for methanol was 8% lower in TBPD than in THPD when the temperature was 90°C. Henry's constants for methanol were statistically different in IL 105, TBPD or THPD, and IL106 with a decreasing order: TBPD or THPD < IL105 < IL106 (p=0.00, 0.00 and 0.00 for IL105 to IL106 at 30°C 60°C and 90°C respectively; p=0.02, 0.00 and 0.00 for IL105 to THPD at 30°C 60°C and 90°C respectively, Figure 20) The difference of Henry's constant among the four ILs increased with increasing temperature (Figure 20). This implies that both TBPD and THPD are the optimum absorbents for methanol among the four RTILs.

4.2.2.2 α-pinene

Henry' constants for α-pinene in the four RTILs are compared in Figure 21. Henry's constants for α-pinene were different at all temperatures. In a increasing order, these were THPD < TBPD < IL105 < IL106 (p=0, for IL105 to IL106 at 30°C; p=0.00 for IL105 to TBPD at each, 30°C, 60°C and 90°C; p=0. for TBPD to THPD at each, 30°C, 60°C and 90°C, Figure 21). The difference between Henry's constants among the four ILs increased with increasing temperature (Figure 21).

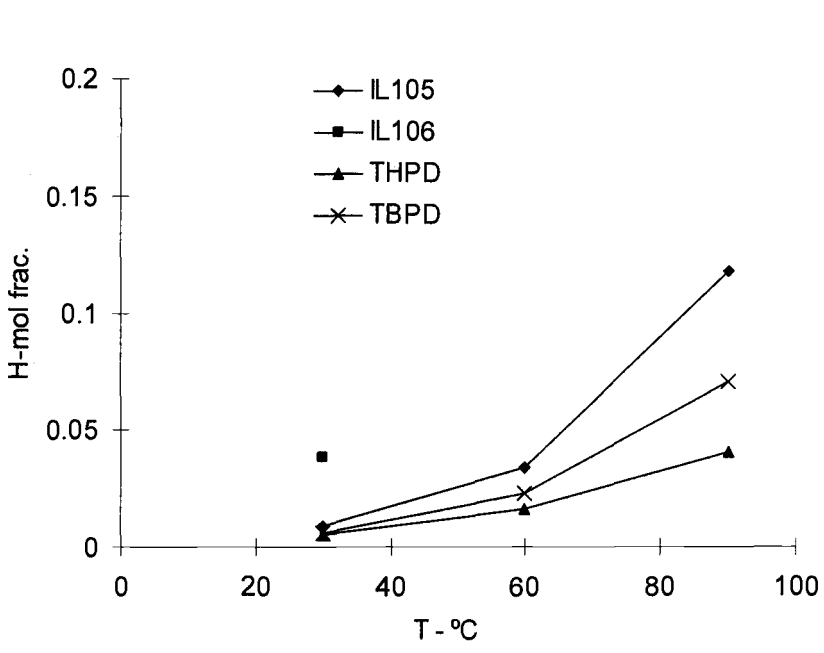

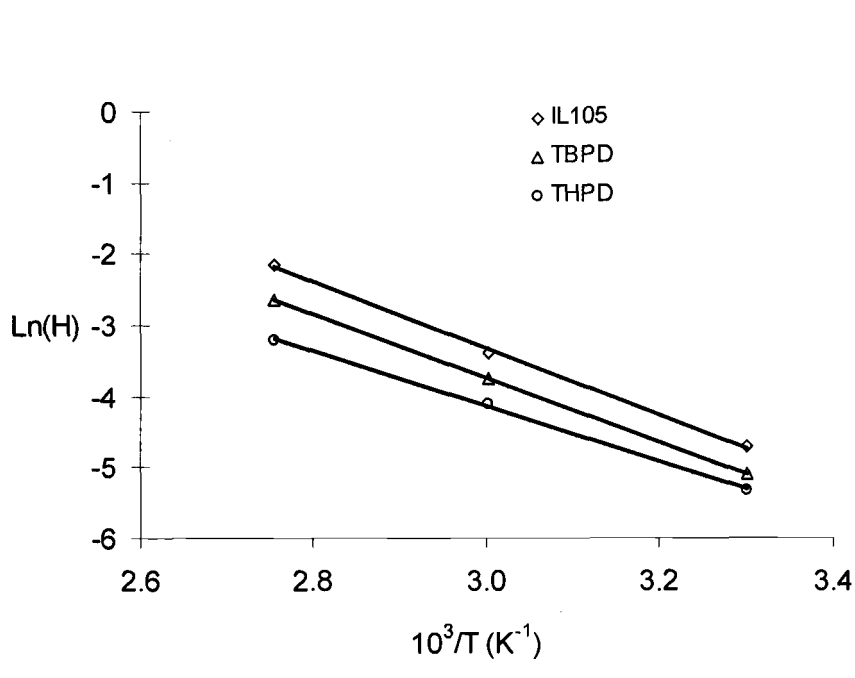

Figure 21. Henry's constant versus temperature (A) and natural log vs. reciprocal absolute temperature (B) for α-pinene in four ILs (Data from α-pinene alone as contaminant: two-component system). Each point is the mean of three data points.

It appeares that THPD was the best absorbent for α-pinene among the four RTILs and then TBPD was the next.

The temperature dependence of Henry's constant means that solubilities of methanol and α-pinene in the four RTILs decreased significantly from 30°C to 90°C the (Figures 16, 17, 18 and 19). At low temperature (30 °C), the differences between the solubilities of methanol and α-pinene is small. The differences increased with increasing temperature due to the high vapor pressure of methanol.

THPD and TBPD should be better absorbents for both methanol and α-pinene, especially at high temperature, than IL105 and IL106. This is directly related to the physiochemical properties of RTILs such as thermal behavior, viscosity, polarity, ionic conductivity. These things are strongly influenced by the structure of the respective ionic species in the ionic liquid. Hiroyuki et al. [50,70] investigated the physicochemical properties and structures of RTILs and concluded that the temperature dependence of ionic diffusivity for RTILs gradually becomes insignificant with increasing volume of cation and anion. Comparing to structures of RTILs 105 and 106, TBPD and THPD have the relatively larger cation or anion. This may explain why temperature had a stronger effect on IL105 and IL106 than on TBPD and THPD. The less effects of temperature on TBPD and THPD allow them good absorbent even at high temperature.

Gas solubility in RTILs is governed by the interaction between the gas molecules and the ions of ionic liquid. The polarization of gases plays an important role in their solubilities. The solubility of methanol, a small, polar molecule and α-pinene, a large, unpolar molecule, can represent the range of common contaminants in the gas stream from wood plants. Anthony et al. [47] studied the effects of anions on gas solubility in ionic liquids and reached a conclusion that the anion appeared to play the most significant role in determining the solubility of gases. The results from our experiment agree with this conclusion that gas solubilities for TBPD and THPD, containing the same anions and different cations are similar, while for IL105 and THPD with the same cations and different anions, the solubilities are significantly different (Figure 20 and 21). This implies that methanol and α-pinene gases had stronger interaction with dodecylbenzenesulfonate anion (TBPD and THPD) than with dicyanamide and tosylate anions (IL105 and IL106).

Increasing the length of an alkyl chain tends to increase the hydrophobic nature of the cation [15], Methanol solubility is lower in THPD than in TBPD because of less hydrogen bonding formed between methanol and THPD (Figure 20). In addition, the higher inductive forces in the RTILs with an increasing number of carbon atoms in the alkyl chain may account for the fact that α-pinene solubility is higher in THPD than TBPD.

Poddar et al. [71] presented measurements of Henry's constants for methanol in high-boiling oils, silicone oil and paratherm. The H values (dimensionless) were 0.069 (31.9 °C) and 0.132 (30 °C) for silicone oil and paratherm respectively. Compared to these data, THPD is better absorbent for methanol (H=0.02, T=30 °C) than silicone oil and paratherm, which are traditional absorbents.

4.2.3 Effects of moisture content on Henry's constant

Although water stable, RTILs are hygroscopic, so the uptake of water vapor from the waste air stream is an important consideration. Henry's constant of methanol and α-pinene in IL105, TBPD, THPD and IL106 were measured at 60 °C in the presence of 2% water based on mass of the absorbent.

4.2.3.1 Methanol

For the four RTILs in this study, the presence of water did change Henry's constant of methanol (Table 14 compared to Table 10-13). Henry's constant for methanol increased significantly in the presence of water (p=0.00 for IL105, p=0.02 for TBPD and p=0.00 for TBPD, Figure 22). Henry's constants for IL106 at 60 °C are not reliable (see Section 4.2.1.4), thus they are not shown in Figure 22.

Table 14. Henry's constants (mol fraction) at 60 °C in the presence of water for methanol and α-pinene in different RTILs.

VOCs		IL105	THPD	TBPD	IL106
methanol	Average	0.0985	0.0833	0.0434	0.1073
	stdev	0.0004	0.0040	0.0003	0.0044
α-pinene	Average	0.0372	0.0187	0.0218	0.0453
	stdev	0.0004	0.0004	0.0010	0.0002

4.2.3.2 α-pinene

Henry's constants for α-pinene in the four RTILs in this study were changed due to the presence of water. Henry's constant for α-pinene in IL105 increased significantly in the presence of water (p=0.01, Figure 23). The data for IL106 may not be reliable and are not shown. However, Henry's constants for α-pinene in TBPD and THPD were not statistically different in the presence of water (p=0.13 for TBPD and p=0.10 for THPD, Figure 23). This would tend to make THPD and TBPD better absorbents for α-pinene in the presence of water than IL105.

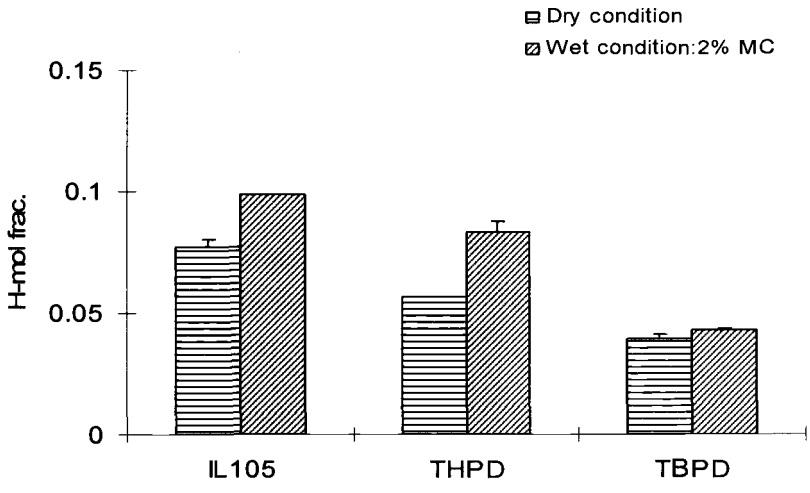

Figure 22. Effect of 2% water on Henry's constant of methanol at 60 °C. The data are the mean of 3 replicates and the error bar represents one standard error of the mean.

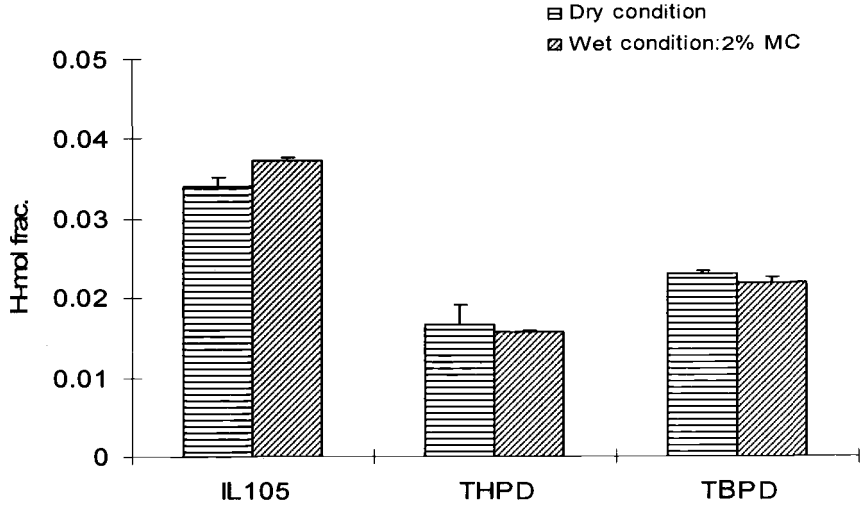

Figure 23. Effect of 2% water on Henry's constants for α-pinene at 60 °C. Each point is the mean of 3 replicates and the error bar represents one standard error of the mean.

The presence of water may significantly affect the properties of RTILs such as thermal stability, viscosity and diffusivity. Water affinity for RTILs varies according to the types of cation and anion [45]. In other words, water will affect differently in different ways, which is consistent with results shown in Figures 22 and 23. Water molecules can form hydrogen-bonding with ions of ILs [47], thus occupy hydrogen-bonding sites, which in turn lead to less hydrogen-bonding between methanol and ILs and decreased the methanol solubility (Figure 22). For α-pinene, hydrogen-bonding is not a concern, which may account for the negligible effects of moisture content on TBPD and THPD.

4.2.4 Absorption of methanol and α-pinene into RTILs in an impinger

In order to imitate the absorption system of industry, methanol and α-pinene were absorbed from a gas stream into RTILs in an impinger continuously.

Henry's constants for methanol and α-pinene based on the impinger method were significantly higher than those based on vial method for both dry and wet conditions ($p < 0.01$ for all comparisons, Figure 24 and Table 15).

A

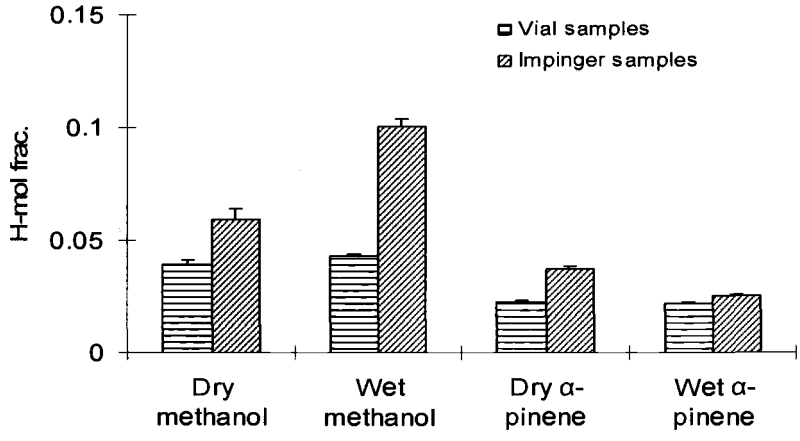

B

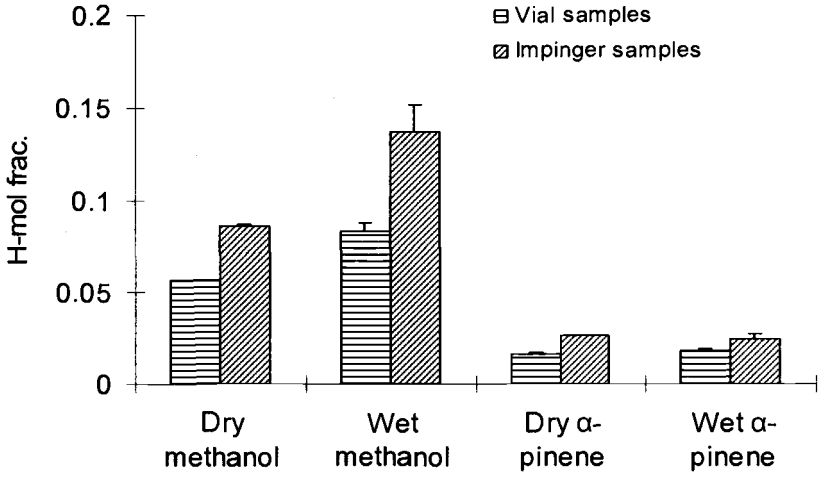

Figure 24. Henry's constant for methanol and α-pinene under wet and dry conditions respectively at 60 °C: TBPD (A) and THPD (B). The wet condition means 2 % water based on mass of RTILs in vials and 20% relative humidity in impinger. The data are the mean of 3 data and the error bar represents one standard error of the mean.

Table 15. Comparison of Henry's constants (mol fraction) between vial and impinger methods.

T = 60 °C			TBPD - H		THPD - H	
			vial	Impinger	vial	Impinger
Dry condition	methanol	mean	0.0393	0.0590	0.0569	0.0857
		stdev	0.0018	0.0042	0.0000	0.0013
	α-pinene	mean	0.0230	0.0372	0.0168	0.0262
		stdev	0.0003	0.0015	0.0004	0.0003
Wet condition	methanol	mean	0.0434	0.1005	0.0833	0.1373
		stdev	0.0003	0.0031	0.0040	0.0128
	α-pinene	mean	0.0218	0.0254	0.0187	0.0250
		stdev	0.0010	0.0004	0.0004	0.0021

There were two sources of uncertainty in our experiments might lead to the difference of Henry's constant based on the vial and the impinger methods. First, the error might have resulted from the uncertainty of the gases bubbled through the impingers. The known concentration gas generated varied 1.5 - 2.9% for methanol and α-pinene (Table 5). Second, the moisture content in air stream was set as 20% RH in the absorbing process of impinger. And the final water content absorbed into RTILs was unknown because the absorption of water was a continuous process. However, the water content into RTILs in vial experiments was designed as 2 wt% based on the mass of RTILs. We speculated that the difference of water content in the two experiments, vial and impinger experiments, also

caused the divergence of their results. The trends are similar for Henry's constants of methanol and α-pinene for both TBPD and THPD so that the same conclusions would be reached regarding the relative absorption capacity of the ILs (Figure 24).

4.2.5 Desorption of methanol and α–pinene from the used RTILs

The desorption of contaminants from RTILs was plotted as function of temperature and vacuum in Figure 25.

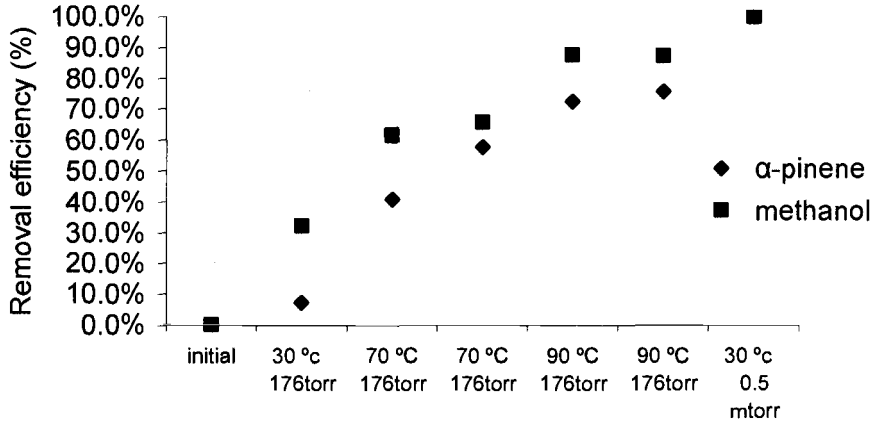

Figure 25. Desorption of methanol and α-pinene from imidazolium-based RTIL (Time for each sample under heat and vacuum is 2 hr; 1torr = 1mmHg = 1000 mtorr).

The removal efficiency of methanol and α-pinene was a function of temperature and vacuum. At the same vacuum, 176 torr, the removal

efficiency of methanol increased from 32% to 86% when the temperature was increased from 30°C to 90°C. However, the removal efficiency was almost up to 100% when the pressure was 0.5 mtorr, even at 30 °C. This indicates that high vacuum is an efficient way to recycle RTILs. Methanol was easier to remove from RTILs than α-pinene due to its lowing boiling point.

Most RTILs have a high viscosity (from 40 to 182 mPa·s at 30°C) due to their low ionic diffusivity [70]. Usually, viscosities of RTILs increase with increasing size of cations and anions. High viscosity has a negative impact on the desorption of contaminants. Tokuda et al. [70] concluded that viscosity was a function of temperature and the viscosity of RTILs decreased significantly with increasing temperature. Low viscosity of RTILs facilitates desorption of contaminates. Therefore, high temperature would improve the removal efficiency of contaminants.

Chapter 6 Conclusions

Henry's Law constant for methanol in imidazolium-based RTILs decreases as the alkyl chain length of the cation increases because the intermolecular interaction of RTIL and methanol increases.

Henry's Law constant is strongly affected by the type of anion. For example, the Henry's Law constant for methanol was much lower for the $[BF_4N_2^-]$ anion than for the $[PF_6^-]$ ion with the $[BMIN^+]$ cation. The $[BF_4N_2^-]$ anion is more hydrophilic than $[PF_6^-]$ and can form more hydrogen-bonding with methanol.

The imidazolium-based ILs are unstable when heated. Evidence of this was a white, pungent gas, probably HF, that was generated. Also, these RTILs etched glassware after desorption at temperatures of 90°C. Therefore, their ability to be reused is limited and they are not desirable for an absorption process. A color change from light yellow to brown or black occurred at a temperature of 90 °C. This may have been the breakdown of α-pinene.

The Henry's Law constants for methanol and α-pinene in phosphonium-based RTILs increased significantly with temperature from 30°C to 90°C. It was demonstrated that this behavior followed the Van't Hoff equation.

The presence of water has a statistically significant, but small effect on some of the Henry's Law constants. The effect is stronger for methanol

than α-pinene. The presence of water increased Henry's Law constant. The Henry's Law constants for α-pinene in TBPD and THPD were not significantly different in the presence of water.

RTILs used to absorb methanol and α-pinene can be recycled under high temperature and vacuum. The removal efficiency can reach 100%. High vacuum appeared to be an effective way to remove contaminates.

This study demonstrated that it is feasible to develop an excellent absorbent for contaminants from wood composite industry based on the data from vial method. Further investigation of the mechanism between gas molecules and ions of RTILs, such as the forces formed among polar and nonpolar gas molecules, cations and anions, may further improve contaminants gases solubility in task-specific RTILs. Results from this study may prompt more research efforts in the development of gas separation using RTILs.

Nomenclature

Symbols

A	GC peak area corresponded to gas sample injected. (μv·s)
A_{H_i}	constant for solvent-solute combination
B_{H_i}	constant for solvent-solute combination
C_g	concentration of contaminant in gas (mole/mole)
$C_{g,m}$	methanol gas concentration. (ppmv)
$C_{g,known}$	gas containing a known concentration contaminant (ppmv)
$C_{g,ppm}$	contaminant gas concentration after dilution, (ppmv)
$C_{g,ppm}'$	contaminant concentration in gas phase (ppmv)
C_L	concentration of contaminant in liquid (mole/mole)
C_L'	concentration of contaminant in gas (mole/L)
C_{Li}	initial concentration liquid (g/g)
$C_{L,ppm}$	concentration of contaminant in liquid (ppmw)
$C_{L.S}$	concentration of contaminant in liquid standards (mol/mol)
C_s	saturated concentration of contaminant gas. (ppmv)
e_S	density of ionic liquid as solvent (g/mL)
K_H	Henry's Law Constant (atm·L / mol)
H	Henry's Law Constant (dimensionless)
m_{IL}	mass of ionic liquid for each liquid sample (g)
M_s	molecular weight of solvent (g/mole)
M_c	molecular weight of contaminant (g/mole)
$M_{c.m}$	molecular weight of methanol (g/mol)
P_{amb}	ambient pressure (Pa)
P_g	vapor pressure of contaminant at the controlled temperature (Pa)
r_m	permeation rate of methanol tube (ng/min)

r_i' actual permeation rate for contaminant gas where i is methanol or α-pinene

R universal gas constant (mL·Pa/mol·K)

RF the slopes of calibration curves, GC response factor (μv·s/ng)

t total running time (min)

T temperature (K)

$V_{\alpha\text{-p}}$ airflow rate through impinger containing α-pinene. (mL/min)

$V_{dilution}$ airflow rate for dilution. (mL/min)

V_i airflow rate through impinger where i is α-pinene and water (mL/min)

$V_{methanol}$ airflow rate through impinger containing methanol. (mL/min)

V_{total} total airflow rate (mL/min)

V_{water} airflow rate through impinger containing water. (mL/min)

W_c weight loss of contaminant (g)

References

1. Nunez, C. 1998. VOCS: Sources, Definitions, and Considerations for Recovery. U.S.EPA National Risk Management Research Laboratory. Cincinnati, OH

2. Hunter, P. and S.T. Oyama. 2000. Absorption. Control of Volatile Organic Compound Emissions: conventional and emerging technologies. John Wiley & Sons, New York. p. 65-93.

3. Milota, M.R.. 2000. Emission from Wood Drying: The science and the issue. Forest Products Journal. 50(6): 10-20.

4. Grosjean D, E.L. Williams, J.H. Seinfeld. 1992. Atmospheric oxidation of selected terpenes and related carbonyls: Gas-phase carbonyl products. Environmental Science and Technology. 26(8):1526–1533.

5. Harley R.A., G.R Cass. 1994. Modelling the concentration of gas-phaseorganic air pollutants: Direct emissions and atmospheric formation. Environmental Science and Technology. 28(1):88–98.

6. U.S. EPA. Jun. 2005. Indoor Air Quality. Sources of Indoor Air Pollution - Organic Gases (Volatile Organic Compounds - VOCs) http://www.epa.gov/iaq/voc.html

7. McGinness, M. 2000. A Novel New Approach to VOC and HAP Emission Control. Proceedings of the Industrial Energy Technology Conference. Houston, Texas.

8. Moretti, E.C. 2002. Reduce VOC and HAP Emissions. Chemical Engineering Progress. 98(6): 30-40.

9. Poddar, T.K., S. Majumdar, and K.K. Sirkar. 1996. Removal of VOCs from air by membrane-based absorption and stripping. Journal of Membrane Science. 120(2): 221-237.

10. Xia, B., S. Majumdar, and K. K. Sirkar. 1999. Regenerative oil scrubbing of volatile organic compounds from a gas stream in hollow fiber membrane devices. Ind. Eng. Chem. Res. 38 (9): 3462-3472

11. Hadjoudj. R., H. Monnier, C. Roizard and F. Lapicque. 2004. Absorption of chlorinated VOCs in high-boiling solvents: determination of Henry's Law Constants and infinite dilution activity coefficients. Ind. Eng. Chem. Res. Vol. 43(9): 2238-2246.

12. Seddon, K.R. 1997. Ionic liquids for clean technology. J. Chem. Tech. Biotechnol. 68: 351-356.

13. Oak Ridge National Laboratory and University of Tennessee. Aug. 2005. Technical Summaries on Ionic Liquids in Chemical Processing. http://www.chemicalvision2020.org/pdfs/tech_summary.pdf

14. Rogers, R.D. and K.R. Seddon. 2002. Ionic liquids-industrial applications to green chemistry. American Chemical Society, Washington D.C.. ACS Symp. Ser. 818. p.2-14.

15. Brennecke J.F., E.J. Maginn. 2001. Ionic liquids: Innovative fluids for chemical processing. AIChE Journal. 47(11): 2384-2389.

16. Forest Products Laboratory. 1999. Wood Handbook—Wood as an engineering material. Gen. Tech. Rep. FPL–GTR–113. Madison, WI: U.S. Department of Agriculture, Forest Service, Forest Products Laboratory. 463 p.

17. Beakler, B.W., P.R. Blankenhorn, L.R. Stover and C.D. Ray. 2005. Total organic compounds released from dehumidification drying of air-dried hardwood lumber. Forest Products Journal. 55(2): 51-61.

18. Rice, R.W. and L. Zibilske. 1999. Estimated VOC losses during the drying of five northeastern species. Forest Products Journal. 49(11/12): 67-70.

19. Barry, A., D. Corneau and R. Lovell. 1999. Press volatile organic compound emissions as a function of wood particleboard processing parameters. Forest Products Journal. 50(10): 35-42.

20. McGinnis, G.D. Dec. 31, 2001. Reducing VOC press emissions from oriented strand board (OSB) manufacturing. Final Project Report. DE-FC07-97EDI 3546. 21 p.

21. Otwell, L.P., M.E. Hittmeier, U. Hooda, H. Yan, W. Su, and S. Banerjee. HAPS release from wood drying. Institute of Paper Science and Technology. IPST Technical Paper Series Number 824. p.1-8.

22. Banerjee, S., W. Su, M.P. Wild, L.P. Otwell, M.E. Hittmeier and K.M. Nichols. 1998. Wet line extension reduce VOCs from softwood drying. Environ. Sci. Technol. 32(9):1303-1307.

23. McDonald, A.G., P. H. Dare, J. S. Gifford, D. Steward and S. Riley 2002. Assessment of air emissions from industrial kiln drying of *Pinus radiata* wood. Holz als Roh- und Werkstoff. 60: 181-190.

24. Heinold, D.W. and T. Hunt. 2003. Wood products MACT risk assessment. Proceedings of TAPPI - Environmental Conference and Exhibit. Portland OR. May 4-7. p.126-137.

25. Punsuvon, V. 1994. Identification of volatile materials emitted during the drying of southern pine lumber. M.S Thesis. Mississippi State University. Mississippi State. Miss. 128 p.

26. National Council for Air and Stream Improvment. 1999. Volatile organic compound emissions from wood products manufacturing facilities. Part V – Oriented Strandboard. Technical bulletin No. 772. NCASI Research Triangle. Park, NC.

27. U.S. EPA. Feb. 1999. The plain English guide to the Clean Air Act. http://www.epa.gov/oar/oaqps/peg_caa/pegcaa02.html

28. U.S. EPA Jul. 2005. Region 8: Maximum Achievable Control Technology. http://www.epa.gov/region08/compliance/mact/mact.html

29. Willingham, R. 2003. Biofiltration Control HAP Emissions from Wood Products Facilities. TAPPI Proceedings - Environmental Conference and Exhibit. p 366-370

30. Federal Register. 2004. National Emission Standards for Hazardous Air Pollutants: Plywood and Composite Wood Products; Effluent Limitations Guidelines and Standards for the Timber Products Point Source Category; List of Hazardous Air Pollutants, Lesser Quantity Designations, Source Category List. Vol. 69, No. 146: 45944 -46045

31. Hunter, P. and S.T. Oyama. 2000. Existing Technoligies for Volatile Organic Compound Elimination. Control of Volatile Organic Compound Emissions: conventional and emerging technologies. John Wiley & Sons, New York. p.18-30.

32. Forestry Products Laboratory. Jul. 2005. Air emissions from wood & wood-based products: air emissions control technologies. http://www.fpl.fs.fed.us/voc/pollcont.html

33. Pond, R.L. 1999. Biofiltration to reduce VOC and HAP emissions in the board industry. Tappi Journal 82(8): 137-140.

34. Milota, M.R. and K. Li. 2001. VOC and HAPs Recovery Using Ionic Liquids. Proposal to DOE 2020 program.

35. Perry, R.H., D.W. Green and J.O. Maloney. 1997. Perry's Chemical Engineer's Handbook, seventh edition. McGraw-Hill. New York. p.14-2.

36. Sauer, B., W. Franklin, R. Miner, D. Word, and B. Upton. 2002. Environmental tradeoffs: life cycle approach to evaluate the burdens and benefits of emission control systems in the wood panel industry. Forest Products Journal 52(3): 50-59.

37. Forsyth, S.A., J.M. Pringle and D.R. MacFarlane. 2004. Ionic liquids-an overview. Australian Journal of Chem. 57: 113-119.

38. Dupont, J., C.S. Consorti and J. Spencer. 2000. Room temperature molten salts: neoteric "Green" solvents for chemical reactions and processes. J. Braz. Chem. Soc. 11(4): 337-344.

39. Rogers, R.D. and K.R. Seddon. 2003. Ionic Liquids as Green Solvents: Progress and Prospects. American Chemical Society, Washington D.C.. ACS Symp. Ser. 856. p.2-12.

40. Earle, M.J. and K.R. Seddon. 2000. Ionic liquids: Green solvents for the future. Pure Appl. Chem. 72 (7): 1391–1398, 2000.

41. Del Sesto, R.E., C. Corley, A. Robertson and J.S. Wilkes. 2005. Tetraalkylphosphonium-based ionic liquids. Journal of Organometallic Chemistry. 690: 2536–2542.

42. Blanchard, L.A. and J.F. Brennecke. 2001. Recovery of organic products from ionic liquids using supercritical carbon dioxide. Ind. Eng. Chem. Res. 40(11): 287-292.

43. Seddon, K.R.. 2001. Catalytic reactions in ionic liquids. Chem. Commun. 2399–2407.

44. Seddon, K.R. 1997. Review: Ionic liquids for clean technology. J. Chem. Tech. Biotechnol. 68:351-356.

45. Anthony, J.L., E.J. Maginn and J.F. Brennecke. 2001. Solution thermodynamics of imidazolium-based ionic liquids and water. J. Phys. Chem. B. 105(44), 10942-10949.

46. Anthony, J.L., E.J. Maginn and J.F. Brennecke. 2002. Solubilities and thermodynamic properties of gas in the ionic liquid 1-n-Butyl-3-methylimidazolium hexafluorophosphate. J. Phys. Chem. B, 106(29):7315- 7320.

47. Anthony, J.L., J.L. Anderson, E.J. Maginn and J.F. Brennecke. 2005. Anion effects on gas solubility in ionic liquids. J. Phys. Chem. B. 109(13): 6366-6374.

48. Rogers, R.D. and K.R. Seddon. 2002. Ionic liquids-industrial applications to green chemistry. American Chemical Society, Washington D.C.. ACS Symp. Ser. 818. p. 247-258.

49. Fredlake, C.P., J.M. Crosthwaite, D.G. Hert, S.N.V.K. Aki and J.F. Brennecke. Thermophysical Properties of Imidazolium-Based Ionic Liquids. Journal of Chemical and Engineering Data. 49(4): 954-964.

50. Tokuda, H., K. Hayamizu, K. Ishii, M.A.B.H. Susan and M. Watanabe. 2005. Physicochemical properties and structures of room temperature ionic liquids. 2. Variation of alkyl chain length in imodazolium cation. J. Phys. Chem. B. 109(13):6103-6110.

51. Bates, E.D., R.D. Mayton, I. Ntai and J.H. Davis. 2002. CO_2 Capture by a task-specific ionic liquid. J. Am. Chem. Soc 124(6): 926-927.

52. Rogers, R.D. and K.R. Seddon. 2002. Ionic liquids-industrial applications to green chemistry, American Chemical Society, Washington D.C.. ACS Symp. Ser. 818. p. 289-307.

53. Rogers, R.D. and K.R. Seddon. 2005. Ionic Liquids IIIB: fundamentals, progress, challenges, and opportunities-transformation and process. p. 49-56.

54. Holbrey, J.D., and K.R. Seddon. 1999. Review:Ionic Liquids. Clean Products and Processes 1: 223–236.

55. Merck. Jun. 2005. Structures. http://pb.merck.de/servlet/PB/menu/1076460/index.html

56. Karodia, N., S. Guise, C. Newlands and J. Andersen. 1998. Clean catalysis with ionic solvents—phosphonium tosylates for hydroformylation. Chem. Commun. 21: 2341-2342.

57. Chen, H., D.C. Kwait, S. Gönen, B.T. Weslowski, D.J. Abdallah and R.G. Weiss. 2002. Phase characterization and properties of completely Saturated quaternary phosphonium salts. Ordered, room-temperature ionic liquids. Chem. Mater. 14(10): 4063-4072

58. Rogers, R.D. and K.R. Seddon. 2002. Ionic liquids-industrial applications to green chemistry, American Chemical Society, Washington D.C.. ACS Symp. Ser. 818. p. 69-85.

59. Baltus, R.E., B.H. Culbertson, D. Sheng, H. Luo and D.W. DePaoli. 2004. Low-pressure solubility of carbon dioxide in room-temperature ionic liquids measured with a quartz crystal microbalance. J. Phys. Chem. B. 108(2): 721-727.

60. Crosthwaite, J. M. and S. N. V. K. Aki. 2004. Liquid phase behavior of imidazolium-based ionic liquids with alcohols. J. Phys. Chem. B. 108(16): 5113-5119

61. Seddon, K.R., A. Stark, and M.J. Torres. 2000. Influence of chloride, water, and organic solvents on the physical properties of ionic liquids. Pure Appl. Chem. 72(12): 2275-2287.

62. Perry, R.H., D.W. Green and J.O. Maloney. 1997. Perry's Chemical Engineer's Handbook, seventh edition. McGraw-Hill. New York. p.4-27.

63. Vu, D.T., P.E. Nicholas, and C.M. Erikson. 2000. SPME/GC-MS characterization of volatiles associated with cocaine and heroin. http://www.americanlaboratory.com/articles/aln/n0009vu.pdf

64. Rocha, S., V. Ramalheira, A. Barros, I. Delgadillo, and M.A. Coimbra. 2001. Headspace solid phase microextraction (SPME) analysis of flavor compounds in wines-effect of the matrix volatile composition in the relative response factors in a wine model. J. Agric. Food Chem. 49(11): 5142-5151.

65. Koziel, J., M. Jia and J. Pawliszyn. 2000. Air sampling with porous solid-phase microextraction fibers. Anal. Chem. 72(21): 5178-5186.

66. Sostaric, T., M.C. Boyce, and E.E. Spickett. 2000. Analysis of the volatile components in vanilla extracts and flavorings by solid-phase

microextraction and gas chromatography. J. Agric. Food Chem. 48(12): 5802-5807.

67. Spinhirne, J.P., J.A. Koziel, and N.K. Chirase. 2004. Sampling and analysis of volatile organic compounds in bovine breath by solid-phase microextraction and gas chromatography–mass spectrometry. Journal of Chromatography A. 1025: 63–69.

68. Lattuati-Derieux, A., S. Bonnassies-Termes, and B. Lavédrine. 2004. Identification of volatile organic compounds emitted by a naturally aged book using solid-phase microextraction/gas chromatography/mass spectrometry. Journal of Chromatography A, 1026: 9–18.

69. Robbins, G.A., S. Wang and J.D. Stuart. 1993. Using the static headspace method to determine Henry's Law constants. Anal. Chem. 65: 3113-3118.

70. Tokuda, H., K. Hayamizu, K. Ishii, M.A.B.H. Susan and M. Watanabe. 2004. Physicochemical properties and structures of room temperature ionic liquids. 1. Variation of anionic species. J. Phys. Chem. B. 108(42):16593-16600.

71. Poddar, T.K. and K.K. Sirkar. 1996. Henry's Law Constant for selected volatile orgainic compounds in high-boiling oils. J. Chem. Eng. Data 41(6): 1329-1332.

Appendix

Table 16. Concentration of methanol and α-pinene in RTIL106.

Temp. (°C)	Methanol		α-pinene		Mix of methanol and α-pinene	
	Conc. (ppmw)		Conc. (ppmw)		Conc. methanol/α-pinene (ppmw)	
	Dry	Wet	Dry	Wet	Dry	Wet
30	183	---	2250	---	183/2250	---
60	27	27	643	643	27/643	27/643
90	12	---	225	---	12/225	12/225

Table 17. Concentration of methanol and α-pinene in TBPD.

Temp. (°C)	Methanol		α-pinene		Mix of methanol and α-pinene	
	Conc. (ppmw)		Conc. (ppmw)		Conc. methanol/α-pinene (ppmw)	
	Dry	Wet	Dry	Wet	Dry	Wet
30	300	---	7500	---	300/7500	---
60	75	75	1875	1875	75/1875	75/1875
90	30	---	750	---	30/750	30/750

Table 18. Concentration of methanol and α-pinene in THPD.

Temp. (°C)	Methanol		α-pinene		Mix of methanol and α-pinene	
	Conc. (ppmw)		Conc. (ppmw)		Conc. methanol/α-pinene (ppmw)	
	Dry	Wet	Dry	Wet	Dry	Wet
30	167	---	11250	---	167/11250	---
60	42	42	2813	2813	42/2813	42/2813
90	17	---	1125	---	17/1125	17/1125

Table 19. The common terms used during calculations through Table 20A to Table 23B.

RF: methanol	6402	(area/ng/inj)
RF: α-pinene	20349	(area/ng/inj)
injection size of gas	0.2	ml
Liquid sample size	0.82	g

Table 20A. Vial experimental parameter and data for RTIL105.

T °C	Sample name	Methanol	α-pinene	GC peak area uv.s		Contaminate Mass in headspace (ng)		H mol frac.	
		(ppmw)	(ppmw)	Methaol	α-pinene	Methaol	α-pinene	Methaol	α-pinene
30	Me-30-1	97.4	0	58873	0	31.796	0	0.021	
	Me-30-2	97.4	0	63765	0	34.438	0	0.023	
	Me-30-3	97.4	0	62182	0	33.583	0	0.023	
60	Me-60-1	28.6	0	60063	0	35.702	0	0.082	
	Me-60-2	28.6	0	61414	0	36.505	0	0.084	
	Me-60-3	28.6	0	60116	0	35.733	0	0.082	
90	Me-90-1	7.8	0	42871	0	25.483	0	0.237	
	Me-90-2	7.8	0	43516	0	25.866	0	0.241	
	Me-90-3	7.8	0	42733	0	25.401	0	0.237	
30	Ap-30-1	0	3750	0	3032850	0	492.868		0.009
	Ap-30-2	0	3750	0	3075300	0	499.767		0.009
	Ap-30-3	0	3750	0	3071696	0	499.181		0.009
60	Ap-60-1	0	1125	0	3233808	0	517.199		0.035
	Ap-60-2	0	1125	0	3009818	0	481.375		0.033
	Ap-60-3	0	1125	0	---	0	---		---
90	Ap-90-1	0	375	0	3362595	0	535.909		0.121
	Ap-90-2	0	375	0	3508891	0	559.225		0.126
	Ap-90-3	0	375	0	3014835	0	480.485		0.108
30	Me,Ap-30-1	97.4	3750	63081	3118599	34.068	506.803	0.023	0.009
	Me,Ap-30-2	97.4	3750	67808	3304195	36.621	536.964	0.025	0.010
	Me,Ap-30-3	97.4	3750	68309	3655067	36.892	593.985	0.025	0.011
60	Me,Ap-60-1	28.6	1125	57497	3130802	34.177	500.725	0.079	0.034
	Me,Ap-60-2	28.6	1125	57700	3220425	34.297	515.058	0.079	0.035
	Me,Ap-60-3	28.6	1125	54156	3036299	32.191	485.610	0.074	0.033
90	Me,Ap-90-1	7.8	375	---	---	---	---	---	---

	Me,Ap-90-2	7.8	375	45094	3460876	26.804	551.573	0.250	0.124
	Me,Ap-90-3	7.8	375	43718	3712398	25.986	591.659	0.242	0.133
60	wet Me-60-1	28.6	0	73756	0	43.841	0	0.101	
	wet Me-60-2	28.6	0	73853	0	43.899	0	0.101	
	wet Me-60-3	28.6	0	78456	0	46.635	0	0.108	
60	wet Ap-60-1	0	1125	0	3526588	0	564.024		0.038
	wet Ap-60-2	0	1125	0	3755035	0	600.561		0.041
	wet Ap-60-3	0	1125	0	3288148	0	525.890		0.036
60	wet Me,Ap-60-1	28.6	1125	72246	3375789	42.944	539.906	0.099	0.037
	wet Me,Ap-60-2	28.6	1125	71632	3457774	42.579	553.019	0.098	0.038
	wet Me,Ap-60-3	28.6	1125	---	---	---	---	---	---
90	wet Me,Ap-90-1	7.8	375	51394	3847111	30.549	613.128	0.286	0.138
	wet Me,Ap-90-2	7.8	375	46652	3511963	27.730	559.715	0.259	0.126
	wet Me,Ap-90-3	7.8	375	57771	3713506	34.340	591.835	0.322	0.133

Note: Density of RTIL105 = 0.89g/mL

Table 20B. Impinger experimental parameter and data for RTIL105.

T- °C	Sample name	methanol	α-pinene	GC peak area (uv.s)		H -mol frac.	
		(ppmw)	(ppmw)	methanol	α-pinene	methanol	α-pinene
60	imp-dry-60-1	73.95287	2259.496	145969	6284763	0.062	0.029
	imp-dry-60-2	53.76958	2275.065	106131	6328070	0.086	0.029
	imp-dry-60-3	101.3101	2185.591	199967	6079198	0.045	0.030
60	imp-wet-60-1	20.81222	1358.693	52350	4126539	0.221	0.048
	imp-wet-60-2	21.23164	1260.267	53405	3827605	0.217	0.052
	imp-wet-60-3	20.81142	1295.353	52348	3934166	0.221	0.051

Table 21A. Vial experimental parameter and data for RTIL106.

T °C	Sample name	methanol (ppmw)	α-pinene (ppmw)	GC peak area (uv.s)		contaminate mass in headspace (ng)		H -mol frac.	
				methanol	α-pinene	methanol	α-pinene	methanol	α-pinene
30	Me-30-1	182.9	0	125383	0	37.041	0.000	0.034	
	Me-30-2	182.9	0	105153	0	31.064	0.000	0.029	
	Me-30-3	182.9	0	109379	0	32.313	0.000	0.030	
60	Me-60-1	27.2	0	49032	0	14.485	0.000	0.100	
	Me-60-2	27.2	0	47434	0	14.013	0.000	0.096	
	Me-60-3	27.2	0	46875	0	13.848	0.000	0.095	
90	Me-90-1	11.6	0	79166	0	23.387	0.000	0.419	
	Me-90-2	11.6	0	78166	0	23.092	0.000	0.414	
	Me-90-3	11.6	0	79066	0	23.358	0.000	0.419	
30	Ap-30-1	0	2250	0	5308065	0.000	482.201		0.037
	Ap-30-2	0	2250	0	5676197	0.000	515.643		0.040
	Ap-30-3	0	2250	0	---	0.000	---		0.000
60	Ap-60-1	0	1285.8	0	3243152	0.000	294.618		0.044
	Ap-60-2	0	1285.8	0	3294789	0.000	299.309		0.044
	Ap-60-3	0	1285.8	0	---	0.000	---		---
90	Ap-90-1	0	225	0	1275404	0.000	115.862		0.108
	Ap-90-2	0	225	0	1323598	0.000	120.240		0.112
	Ap-90-3	0	225	0	---	0.000	---		---
30	Me,Ap-30-1	182.9	2250	99914	3166240	29.517	287.631	0.027	0.022
	Me,Ap-30-2	182.9	2250	103446	3256315	30.560	295.813	0.028	0.023
	Me,Ap-30-3	182.9	2250	---	---	---	---	---	---
60	Me,Ap-60-1	27.2	1285.8	63836	1555457	18.858	141.302	0.130	0.021
	Me,Ap-60-2	27.2	1285.8	71505	1674444	21.124	152.112	0.146	0.023
	Me,Ap-60-3	27.2	1285.8	63031	1361775	18.621	123.708	0.128	0.018
90	Me,Ap-90-1	11.6	225	54427	1240406	16.079	112.682	0.262	0.096
	Me,Ap-90-2	11.6	225	53861	1353857	15.912	122.988	0.283	0.114

	Me,Ap-90-3	11.6	225	54605	1387598	16.131	126.054	0.287	0.117
60	wet Me-60-1	27.2	0	45158	0	13.341	0.000	0.092	
	wet Me-60-2	27.2	0	---	0	---	0.000	---	
	wet Me-60-3	27.2	0	45556	0	13.458	0.000	0.093	
60	wet Ap-60-1	0	1285.8	0	7479007	0.000	679.416		0.101
	wet Ap-60-2	0	1285.8	0	7817229	0.000	710.141		0.106
	wet Ap-60-3	0	1285.8	0	7200829	0.000	654.145		0.097
60	wet Me,Ap-60-1	27.2	1285.8	50582	3344902	14.943	303.861	0.103	0.045
	wet Me,Ap-60-2	27.2	1285.8	54899	3370950	16.218	306.227	0.112	0.045
	wet Me,Ap-60-3	27.2	1285.8	52741	3357925	15.55	305.1	0.106	0.044
90	wet Me,Ap-90-1	11.6	225	---	1343919	---	122.086	---	0.113
	wet Me,Ap-90-2	11.6	225	62068	1250770	18.336	113.624	0.327	0.105
	wet Me,Ap-90-3	11.6	225	61439	1125628	18.150	102.255	0.324	0.095

Note: Density of RTIL106 =0.89g/mL

Table 21B. Impinger experimental parameter and data for RTIL106.

T °C	Sample name	methanol	α-pinene	GC peak area (uv.s)		H -mol frac.	
		(ppmw)	(ppmw)	methanol	α-pinene	methanol	α-pinene
60	imp-dry-60-1	38.78933	1533.684	94298	1825629	0.168	0.061
	imp-dry-60-2	41.90077	1452.467	101862	1728952	0.155	0.064
	imp-dry-60-3	44.27219	1514.552	107627	1802855	0.147	0.061
60	imp-wet-60-1	48.29682	2307.638	93647	6026503	0.135	0.040
	imp-wet-60-2	43.85997	2539.848	85044	6632931	0.149	0.037
	imp-wet-60-3	47.33962	2492.854	91791	6510202	0.138	0.037

Table 22A. Vial experimental parameter and data for TBPD.

T °C	Sample name	methanol (ppmw)	α-pinene (ppmw)	GC peak area (uv.s)		contaminant mass in headspace (ng)		H -mol frac.	
				methanol	α-pinene	methanol	α-pinene	methanol	α-pinene
30	Me-30-1	300	0	222906	0	65.851	0.000	0.020	
	Me-30-2	300	0	---	0	---	0.000	---	
	Me-30-3	300	0	222800	0	65.820	0.000	0.020	
60	Me-60-1	75	0	184909	0	54.626	0.000	0.073	
	Me-60-2	75	0	166639	0	49.229	0.000	0.066	
	Me-60-3	75	0	165630	0	48.931	0.000	0.066	
90	Me-90-1	30	0	182636	0	53.955	0.000	0.200	
	Me-90-2	30	0	170535	0	50.380	0.000	0.186	
	Me-90-3	30	0	176678	0	52.194	0.000	0.193	
30	Ap-30-1	0	7500	0	5294032	0.000	480.926		0.006
	Ap-30-2	0	7500	0	5592739	0.000	508.061		0.006
	Ap-30-3	0	7500	0	---	0.000	---		---
60	Ap-60-1	0	1875	0	4808370	0.000	436.807		0.024
	Ap-60-2	0	1875	0	---	0.000	---		---
	Ap-60-3	0	1875	0	4568478	0.000	415.014		0.023
90	Ap-90-1	0	750	0	5076154	0.000	461.133		0.069
	Ap-90-2	0	750	0	5230043	0.000	475.113		0.071
	Ap-90-3	0	750	0	5367845	0.000	487.631		0.073
30	Me,Ap-30-1	300	7500	0	5522660	0.000	501.695		0.011
	Me,Ap-30-2	300	7500	80024	---	23.641	---	---	0.006
	Me,Ap-30-3	300	7500	84014	5229181	24.819	475.035	0.007	0.000
60	Me,Ap-60-1	75	1875	104410	4565922	30.845	414.782	0.007	0.006
	Me,Ap-60-2	75	1875	98609	4654941	29.131	422.869	0.041	0.023
	Me,Ap-60-3	75	1875	95673	4702596	28.264	427.198	0.039	0.023
60	Me,Ap-90-1	30	750	108289	4585585	32.0	416.6	0.039	0.023
	Me,Ap-90-2	30	750	113221	4546555	33.448	413.023	0.108	0.057

	Me,Ap-90-3	30	750	104698	4632372	30.930	420.819	0.123	0.062
60	wet Me-60-1	75	0	180904	0	53.443	0.000	0.072	
	wet Me-60-2	75	0	---	0	---	0.000	0.000	
	wet Me-60-3	75	0	182748	0	53.988	0.000	0.072	
60	wet Ap-60-1	0	1875	0	4570803	0.000	415.226		0.023
	wet Ap-60-2	0	1875	0	4655711	0.000	422.939		0.023
	wet Ap-60-3	0	1875	0	4667087	0.000	423.972		0.023
60	wet Me,Ap-30-1	300	7500	46114	5421879	13.623	492.540	0.004	0.006
	wet Me,Ap-30-2	300	7500	54578	6387386	16.123	580.249	0.005	0.007
	wet Me,Ap-30-3	300	7500	---	---	---	---	---	---
90	wet Me,Ap-60-1	75	1875	109267	4300049	32.280	390.629	0.043	0.021
	wet Me,Ap-60-2	75	1875	110791	4300049	32.730	390.629	0.044	0.021
	wet Me,Ap-60-3	75	1875	119457	4634539	35.290	421.016	---	0.023
60	wet Me,Ap-90-1	30	750	84210	4662188	24.877	423.527	0.091	0.063
	wet Me,Ap-90-2	30	750	75149	4495756	22.201	408.408	0.081	0.061
	wet Me,Ap-90-3	30	750	65383	4572405	19.316	415.371	0.070	0.062

Note: Density of TBPD = 0.95g/mL

Table 22B. Impinger experimental parameter and data for TBPD.

T °C	Sample name	methanol	α-pinene	GC peak area (uv.s)		H -mol frac.	
		(ppmw)	(ppmw)	methanol	α-pinene	methanol	α-pinene
60	imp-dry-60-1	52.22364	1409.337	69353	3488505	0.055	0.039
	imp-dry-60-2	45.32605	1449.713	60193	3588447	0.063	0.037
	imp-dry-60-3	48.95407	1529.455	65011	3785832	0.059	0.035
60	imp-wet-60-1	29.49927	2171.203	43277	5173015	0.097	0.025
	imp-wet-60-2	27.71542	2099.531	40660	5002253	0.104	0.026
	imp-wet-60-3	---	---	---	---	---	---

Table 23A. Vial experimental parameter and data for THPD.

T °C	Sample name	methanol (ppmw)	α-pinene (ppmw)	GC peak area (uv.s) methanol	GC peak area (uv.s) α-pinene	contaminant mass in headspace (ng) methanol	contaminant mass in headspace (ng) α-pinene	H -mol frac. methanol	H -mol frac. α-pinene
30	Me-30-1	166.7	0	138354	0	40.873	0	0.020	---
	Me-30-2	166.7	0	142124	0	41.986	0	0.021	
	Me-30-3	166.7	0	134584	0	39.759	0	0.019	
60	Me-60-1	41.7	0	---	0	---	0	0.000	
	Me-60-2	41.7	0	100039	0	29.554	0	0.064	
	Me-60-3	41.7	0	97213	0	28.719	0	0.062	
90	Me-90-1	16.7	0	118859	0	35.113	0	0.210	
	Me-90-2	16.7	0	119786	0	35.387	0	0.212	
	Me-90-3	16.7	0	---	0	---	0	---	
30	Ap-30-1	0	11250	0	7317296	0.000	664.725		0.005
	Ap-30-2	0	11250	0	7197230	0.000	653.818		0.005
	Ap-30-3	0	11250	0	7249351	0.000	658.553		0.005
60	Ap-60-1	0	2812.5	0	5746549	0.000	522.034		0.017
	Ap-60-2	0	2812.5	0	5590559	0.000	507.770		0.017
	Ap-60-3	0	2812.5	0	5434761	0.000	493.710		0.016
90	Ap-90-1	0	1125	0	---	0.000	---		---
	Ap-90-2	0	1125	0	5128576	0.000	465.895		0.041
	Ap-90-3	0	1125	0	4992505	0.000	453.534		0.040
30	Me,Ap-30-1	166.7	11250	104027	7599115	30.732	690.327	0.015	0.005
	Me,Ap-30-2	166.7	11250	101001	700895	29.680	637.012	0.014	0.005
	Me,Ap-30-3	166.7	11250	96875	6427760	28.619	583.917	0.014	0.004
60	Me,Ap-60-1	41.7	2812.5	89361	5540829	26.399	503.346	0.057	0.016
	Me,Ap-60-2	41.7	2812.5	89219	5792360	26.357	526.195	0.057	0.017

	Me,Ap-60-3	41.7	2812.5	---	---	---	---	---	---
60	Me,Ap-90-1	16.7	1125	120596	7355439	35.627	668.190	0.196	0.055
	Me,Ap-90-2	16.7	1125	118868	5824035	35.116	529.073	0.210	0.047
	Me,Ap-90-3	16.7	1125	134918	6822247	39.858	619.754	0.240	0.055
60	wet Me-60-1	41.7	0	182021	0	53.773	0.000	0.117	
	wet Me-60-2	41.7	0	178202	0	52.620	0.000	0.115	
	wet Me-60-3	41.7	0	---	0	---	0.000	0.000	
60	wet Ap-60-1	0	2812.5	0	5188880	0.000	471.374		0.015
	wet Ap-60-2	0	2812.5	0	5409905	0.000	490.756		0.016
	wet Ap-60-3	0	2812.5	0	5640703	0.000	512.419		0.017
60	wet Me,Ap-60-1	41.7	2812.5	136364	6447228	40.285	585.686	0.087	0.019
	wet Me,Ap-60-2	41.7	2812.5	123998	6189084	36.632	562.235	0.079	0.018
	wet Me,Ap-60-3	41.7	2812.5	---	---	---	---	---	---
90	wet Me,Ap-90-1	16.7	1125	145118	8319795	42.871	755.795	0.258	0.067
	wet Me,Ap-90-2	16.7	1125	140700	8306301	41.566	754.569	0.250	0.067
	wet Me,Ap-90-3	16.7	1125	154675	8312918	45.694	755.09	0.276	0.000

Table 23B. Impinger experimental parameter and data for THPD.

T °C	Sample name	methanol	α-pinene	GC peak area (uv.s)		H -mol frac.	
		(ppmw)	(ppmw)	methanol	α-pinene	methanol	α-pinene
60	imp-dry-60-1	28.65573	1855.398	61359	3738236	0.087	0.026
	imp-dry-60-2	29.54867	1899.64	63271	3827375	0.084	0.026
	imp-dry-60-3	---	---	---	---	---	---
60	imp-wet-60-1	18.1335	1408.402	56610	3163912	0.138	0.027
	imp-wet-60-2	16.62766	1579.88	51909	3549130	0.150	0.024
	imp-wet-60-3	20.05992	1651.548	62624	3710128	0.124	0.023

Note: Density of THPD = 0.93g/mL